

Efficient Global Optimization of Two-layer ReLU Networks: Quadratic-time Algorithms and Adversarial Training*

Yatong Bai[†], Tanmay Gautam[‡], and Somayeh Sojoudi[§]

Abstract. The non-convexity of the artificial neural network (ANN) training landscape brings inherent optimization difficulties. While the traditional back-propagation stochastic gradient descent (SGD) algorithm and its variants are effective in certain cases, they can become stuck at spurious local minima and are sensitive to initializations and hyperparameters. Recent work has shown that the training of an ANN with ReLU activations can be reformulated as a convex program, bringing hope to globally optimizing interpretable ANNs. However, naively solving the convex training formulation has an exponential complexity, and even an approximation heuristic requires cubic time. In this work, we characterize the quality of this approximation and develop two efficient algorithms that train ANNs with global convergence guarantees. The first algorithm is based on the alternating direction method of multiplier (ADMM). It solves both the exact convex formulation and the approximate counterpart. Linear global convergence is achieved, and the initial several iterations often yield a solution with high prediction accuracy. When solving the approximate formulation, the per-iteration time complexity is quadratic. The second algorithm, based on the “sampled convex programs” theory, is simpler to implement. It solves unconstrained convex formulations and converges to an approximately globally optimal classifier. The non-convexity of the ANN training landscape exacerbates when adversarial training is considered. We apply the robust convex optimization theory to convex training and develop convex formulations that train ANNs robust to adversarial inputs. Our analysis explicitly focuses on one-hidden-layer fully connected ANNs, but can extend to more sophisticated architectures.

Key words. Robust Optimization, Convex Optimization, Adversarial Training, Neural Networks

AMS subject classifications. 68Q25, 82C32, 49M29, 46N10, 62M45

1. Introduction. The artificial neural network (ANN) is one of the most powerful and popular machine learning tools. Optimizing a typical ANN with non-linear activation functions and a finite width requires solving non-convex optimization problems. Traditionally, training ANNs relies on stochastic gradient descent (SGD) back-propagation [47]. While SGD back-propagation has seen a tremendous empirical success, it is only guaranteed to converge to a local minimum when applied to the non-convex ANN training objective. While SGD back-propagation can converge to a global optimizer for one-hidden-layer “rectified linear unit (ReLU)”-activated networks when the considered network is wide enough [39, 20] or when the inputs follow a Gaussian distribution [15], spurious local minima can exist in gen-

*This work is an extension of [9].

Funding: This work was supported by grants from ONR and NSF.

[†]Department of Mechanical Engineering, University of California, Berkeley, (yatong_bai@berkeley.edu).

[‡]Department of Electrical Engineering and Computer Science, University of California, Berkeley, (tgautam23@berkeley.edu).

[§]Department of Mechanical Engineering and Department of Electrical Engineering and Computer Science, University of California, Berkeley, (sojoudi@berkeley.edu).

eral applications. Moreover, the non-convexity of the training landscape and the properties of back-propagation SGD cause the issues listed below:

- **Poor interpretability:** With SGD, it is hard to monitor the training status. For example, when the progress slows down, we may or may not be close to a local minimum, and the local minimum may be spurious.
- **High sensitivity to hyperparameters:** Back-propagation SGD has several important hyperparameters to tune. Every parameter is crucial to the performance, but selecting the parameters can be difficult. SGD is also sensitive to the initialization [28].
- **Vanishing / exploding gradients:** With back-propagation, the gradient at shallower layers can be tiny (or huge) if the deeper layer weights are tiny (or huge).

While more advanced back-propagation optimizers such as Adam [36] can alleviate the above issues, avoiding them entirely can be hard. Since convex programs possess the desirable property that all local minima are global, the existing works have considered convexifying the ANN training problem [12, 8, 6]. More recently, Pilanci and Ergen proposed “convex training” and derived a convex optimization problem with the same global minimum as the non-convex cost function of a one-hidden-layer fully-connected ReLU ANN, enabling global ANN optimization [45]. The favorable properties of convex optimization make convex training immune to the deficiencies of back-propagation. Convex training also extends to more complex ANNs such as convolutional neural networks (CNNs) [24], deeper networks [23], and vector-output networks [48]. This work starts with one-hidden-layer ANNs for simplicity. In Appendix D.2, we show the possibilities of extending to more complex ANNs. One-hidden-layer networks are the simplest ANN instances possessing the vast representation power of ANNs [31], and their theoretical analysis helps with understanding more complex networks [20, 52].

Unfortunately, the $\mathcal{O}(d^3 r^3 (\frac{n}{r})^{3r})$ computational complexity of the convex training formulation introduced in [45] is prohibitively high. This complexity arises due to the following two reasons:

- The size of the convex program grows exponentially in the training data matrix rank r . This exponential relationship is inherent due to the large number of possible ReLU activation patterns, and thus can be hard to reduce. Fortunately, this problem is not a deal-breaker in practice: [45] has shown that a heuristic approximation that forms much smaller convex optimizations performs surprisingly well. In this work, we analyze this approximation and theoretically show that for a given level of suboptimality, the required size of the convex training programs is linear in the number of training data points n .
- The convex training formulation is constrained. The naive choice of algorithm for solving a constrained convex optimization is often the interior-point method (IPM), which has a cubic per-step computational complexity. This paper develops more efficient algorithms that exploit the problem structure and achieve lower computational cost. Specifically, an algorithm based on the alternating direction method of multipliers (ADMM) with a quadratic per-iteration complexity, as well as a Sampled Convex Program (SCP)-based algorithm with a linear per-iteration complexity, are introduced.

Detailed comparisons among the ADMM-based algorithm, the SCP-based algorithm, the original convex training algorithm in [45], and back-propagation SGD are presented in Table 1.

| Method | Complexity | Global convergence |
|----------------------|--|---|
| IPM [45] | $\mathcal{O}(d^3 r^3 (\frac{n}{r})^{3r})^\dagger$ | Superlinear to the global optimum. |
| ADMM (exact) | $\mathcal{O}(d^2 r^2 (\frac{n}{r})^{2r})^\dagger$ | Rapid to a moderate accuracy; linear to the global optimum. |
| ADMM (approximate) | $\mathcal{O}(n^2 d^2)^\S$ | Rapid to a moderate accuracy; linear to an approximate global optimum. |
| SCP | $\mathcal{O}(n^2)^\S$ | Towards an approximate global optimum; $\mathcal{O}(1/T)$ rate for weakly convex loss; linear for strongly convex loss. |
| SGD back-propagation | $\mathcal{O}(mnd)^\ddagger / \mathcal{O}(n^2 d)^\dagger$ | No spurious valleys if $m \geq 2n + 2$; no general results. |

Table 1: Comparisons between the proposed ANN training methods and related methods. The middle column is the per-epoch complexity when the squared loss is considered. n is the number of training points; d is the data dimension; r is the training data matrix rank.

\dagger : Towards the theoretically lowest loss – further increasing network width will not reduce the training loss;

\S : Towards a fixed desired level of suboptimality in the sense defined in [Theorem 2.2](#);

\ddagger : For an arbitrary network width m . Since there exists a globally optimal neural network with no more than $n + 1$ active hidden-layer neuron [39], the $\mathcal{O}(mnd)$ bound for SGD back-propagation evaluates to $\mathcal{O}(n^2 d)$.

While IPM can converge to a highly accurate solution with less iterations, ADMM can rapidly reach a medium-precision solution, which is often sufficient for machine learning tasks. Compared with SGD back-propagation, ADMM has a higher theoretical complexity but is guaranteed to linearly converge to a global optimum, enabling efficient global convergence.

Prior literature has considered applying the ADMM method to ANN training [51, 53]. These works used ADMM to separate the activations and the weights of each layer, enabling parallel computing. While the ADMM algorithm in [53] converges at an $\mathcal{O}(1/t)$ rate (t is the number of iterations) to a critical point of the augmented Lagrangian of the training formulation, there is no guarantee that this critical point is a global optimizer of the ANN training loss. In contrast, this paper uses ADMM as an efficient convex optimization algorithm and introduces an entirely different splitting scheme based on the convex formulations conceived in [45]. More importantly, our ADMM algorithm provably converges to a globally optimal classifier.

Combining the SCP analysis and the convex training framework leads to a further simplified convex training program that solves unconstrained convex optimizations. This SCP-based method converges to an approximate global optimum. The scale of the SCP convex training formulation can be larger than the convex problem solved in the ADMM algorithm. However, the unconstrained nature enables the use of gradient methods, whose per-iteration complexities are lower than ADMM. The similarities between the SCP-based algorithm and extreme learning machines (ELMs) [32, 25] show that the training of a sparse ELM can be regarded as a convex relaxation of the training of an ANN, providing insights into the hidden sparsity

of neural networks. Due to space restrictions, this result is presented in [Appendix A](#).

More recently, [11] designed a layer-wise training scheme that concatenates one-hidden-layer ANNs into a deep network, where each layer reduces the training error. This concatenation approach can be combined with the convex training of one-hidden-layer ANNs discussed in this work, ultimately leading to training deep networks with convex optimization.

Neural networks can be vulnerable to adversarial attacks. Such a vulnerability has been observed in the field of computer vision [50, 44, 26] and controls [34]. While there have been studies on robustness certification [2, 42, 4] and achieving certified robustness at test time via “randomized smoothing” [18, 3], efficiently achieving robustness via training remains an important topic. To this end, “adversarial training” [38, 26, 33] is one of the most effective methods to obtain robust classifiers via training, compared with other methods such as obfuscated gradients [7]. Specifically, adversarial training replaces the standard loss function with an “adversarial loss” and solves a bi-level mini-max optimization to train robust ANNs.

When adversarial training is considered, the aforementioned issues of SGD back-propagation become worse: adversarial training can be highly unstable in practice, and convergence properties are pessimistic. Therefore, extending convex training to adversarial training is crucial. In our conference version [9], we built upon the above results to develop “convex adversarial training”, explicitly focusing on the cases of hinge loss (for binary classification) and squared loss (for regression). We theoretically showed that solving the proposed robust convex optimizations trains robust ANNs and empirically demonstrated the efficacy and advantages over traditional methods. This work extends the analysis to the binary cross-entropy loss and discusses the extensibility to more complex ANN architectures.

Previously, researchers have applied convex relaxation techniques to adversarial training. These works obtain convex certifications (semi-definite program (SDP) [46] or linear program (LP) [54]) that upper-bound the inner maximization of the adversarial training formulation and use weak duality to develop robust loss functions. Note that while these works use convex relaxation, the resulting training formulations are still non-convex. Furthermore, since multiple layers of relaxations stack together in these works, the analysis can be too conservative. In contrast, we apply robust optimization techniques to the entire mini-max adversarial training formulation and obtain convex training problems.

1.1. Notations. Throughout this work, we focus on fully-connected ANNs with one ReLU-activated hidden layer and a scalar output, defined as

$$\hat{y} = \sum_{j=1}^m (Xu_j + b_j \mathbf{1}_n)_+ \alpha_j,$$

where $X \in \mathbb{R}^{n \times d}$ is the input data matrix with n data points in \mathbb{R}^d and $\hat{y} \in \mathbb{R}^n$ is the output vector of the ANN. We denote the target output used for training as $y \in \mathbb{R}^n$. The vectors $u_1, \dots, u_m \in \mathbb{R}^d$ are the weights of the m neurons in the hidden layer while the scalars $\alpha_1, \dots, \alpha_m \in \mathbb{R}$ are the weights of the output layer. $b_1, \dots, b_m \in \mathbb{R}$ are the hidden layer bias terms. The symbol $(\cdot)_+ = \max\{0, \cdot\}$ indicates the ReLU activation function which sets all negative entries of a vector or a matrix to zero. The symbol $\mathbf{1}_n$ defines a column vector

with all entries being 1, where the subscript n denotes the dimension of this vector. The n -dimensional identity matrix is denoted by I_n .

Furthermore, for a vector $q \in \mathbb{R}^n$, $\text{sgn}(q) \in \{-1, 0, 1\}^n$ denotes the signs of the entries of q . $[q \geq 0]$ denotes a boolean vector in $\{0, 1\}^n$ with ones at the locations of the nonnegative entries of q and zeros at the remaining locations. The symbol $\text{diag}(q)$ denotes a diagonal matrix $Q \in \mathbb{R}^{n \times n}$ where $Q_{ii} = q_i$ for all i and $Q_{ij} = 0$ for all $i \neq j$. For a vector $q \in \mathbb{R}^n$ and a scalar $b \in \mathbb{R}$, the inequality $q \geq b$ means that $q_i \geq b$ for all $i \in [n]$. The symbol \odot denotes the Hadamard product between two vectors with same dimensionalities. The notation $\|\cdot\|_p$ denotes the ℓ_p -norm within \mathbb{R}^n . For a matrix A , the max norm $\|A\|_{\max}$ is defined as $\max_{ij} |a_{ij}|$, where a_{ij} is the entry at the location (i, j) .

Moreover, for a set \mathcal{A} , the notation $|\mathcal{A}|$ denotes its cardinality, and $\Pi_{\mathcal{A}}(\cdot)$ denotes the projection onto \mathcal{A} . The notation prox_f denotes the proximal operator associated with a function $f(\cdot)$. The notation $R \sim \mathcal{N}(0, I_n)$ indicates that a random variable $R \in \mathbb{R}^n$ is a standard normal random vector, and $\text{Unif}(\mathcal{S}^{n-1})$ denotes the uniform distribution on a $(n - 1)$ -sphere. For $P \in \mathbb{N}_+$, we define $[P]$ as the set $\{a \in \mathbb{N}_+ | a \leq P\}$, where \mathbb{N}_+ is the set of positive integers.

2. Practical Convex ANN Training.

2.1. Prior work – convex ANN training. We define the problem of training the above ANN with an ℓ_2 regularized convex loss function $\ell(\hat{y}, y)$ as:

$$\min_{(u_j, \alpha_j, b_j)_{j=1}^m} \ell \left(\sum_{j=1}^m (Xu_j + b_j \mathbf{1}_n)_+ \alpha_j, y \right) + \frac{\beta}{2} \sum_{j=1}^m \left(\|u_j\|_2^2 + b_j^2 + \alpha_j^2 \right).$$

where $\beta > 0$ is a regularization parameter. Without loss of generality, we assume that $b_j = 0$ for all $j \in [m]$. We can safely make this simplification because concatenating a column of ones to the data matrix X absorbs the bias terms. The simplified training problem is then:

$$(2.1) \quad \min_{(u_j, \alpha_j)_{j=1}^m} \ell \left(\sum_{j=1}^m (Xu_j)_+ \alpha_j, y \right) + \frac{\beta}{2} \sum_{j=1}^m \left(\|u_j\|_2^2 + \alpha_j^2 \right).$$

Consider a set of diagonal matrices $\{\text{diag}([Xu \geq 0]) | u \in \mathbb{R}^d\}$, and let the distinct elements of this set be denoted as D_1, \dots, D_P . The constant P corresponds to the total number of partitions of \mathbb{R}^d by hyperplanes passing through the origin that are also perpendicular to the rows of X [45]. Intuitively, P can be regarded as the number of possible ReLU activation patterns associated with X .

Consider the convex optimization problem

$$(2.2) \quad \min_{(v_i, w_i)_{i=1}^P} \ell \left(\sum_{i=1}^P D_i X(v_i - w_i), y \right) + \beta \sum_{i=1}^P \left(\|v_i\|_2 + \|w_i\|_2 \right)$$

s. t. $(2D_i - I_n)Xv_i \geq 0, (2D_i - I_n)Xw_i \geq 0, \quad \forall i \in [P]$

Algorithm 2.1 Practical convex training

1: Generate P_s distinct diagonal matrices via $D_h \leftarrow \text{diag}([Xa_h \geq 0])$, where $a_h \sim \mathcal{N}(0, I_d)$ i.i.d. for all $h \in [P_s]$.

2: Solve

$$(2.5) \quad p_{s1}^* = \min_{(v_h, w_h)_{h=1}^{P_s}} \ell \left(\sum_{h=1}^{P_s} D_h X(v_h - w_h), y \right) + \beta \sum_{h=1}^{P_s} (\|v_h\|_2 + \|w_h\|_2)$$

$$\text{s. t. } (2D_h - I_n)Xv_h \geq 0, (2D_h - I_n)Xw_h \geq 0, \quad \forall h \in [P_s].$$

3: Recover u_1, \dots, u_{m_s} and $\alpha_1, \dots, \alpha_{m_s}$ from the solution $(v_{s_h}^*, w_{s_h}^*)_{h=1}^{P_s}$ of (2.5) using (2.4).

and its dual formulation

$$(2.3) \quad \max_v -\ell^*(v) \quad \text{s. t. } |v^\top (Xu)_+| \leq \beta, \quad \forall u : \|u\|_2 \leq 1$$

where $\ell^*(v) = \max_z z^\top v - \ell(z, y)$ is the Fenchel conjugate function. Note that (2.3) is a convex semi-infinite program. The next theorem borrowed from Pilanci and Ergen's paper [45] explains the relationship between the non-convex training problem (2.1), the convex problem (2.2), and the dual problem (2.3) when the ANN is sufficiently wide.

Theorem 2.1 ([45]). *Let $(v_i^*, w_i^*)_{i=1}^P$ denote a solution of (2.2) and define m^* as $|\{i : v_i^* \neq 0\}| + |\{i : w_i^* \neq 0\}|$. Suppose that the ANN width m is at least m^* , where m^* is upper-bounded by $n + 1$. If the loss function $\ell(\cdot, y)$ is convex, then (2.1), (2.2), and (2.3) share the same optimal objective. The optimal network weights $(u_j^*, \alpha_j^*)_{j=1}^m$ can be recovered using the formulas*

$$(2.4) \quad (u_{j_{1i}}^*, \alpha_{j_{1i}}^*) = \left(\frac{v_i^*}{\sqrt{\|v_i^*\|_2}}, \sqrt{\|v_i^*\|_2} \right) \quad \text{if } v_i^* \neq 0;$$

$$(u_{j_{2i}}^*, \alpha_{j_{2i}}^*) = \left(\frac{w_i^*}{\sqrt{\|w_i^*\|_2}}, -\sqrt{\|w_i^*\|_2} \right) \quad \text{if } w_i^* \neq 0.$$

where the remaining $m - m^*$ neurons are chosen to have zero weights.

The worst-case computational complexity of solving (2.2) for the case of squared loss is $\mathcal{O}(d^3 r^3 (\frac{n}{r})^{3r})$ using standard interior-point solvers [45]. Here, r is the rank of the data matrix X and in many cases $r = d$. Such complexity is polynomial in n but exponential in r . This complexity is already a significant improvement over previous methods but still prohibitively high for many practical applications. Such high complexity is due to the large number of D_i matrices, which is upper-bounded by $\min \{2^n, 2r (\frac{e(n-1)}{r})^r\}$ [45].

2.2. A practical algorithm for convex training. A natural direction of mitigating this high complexity is to reduce the number of D_i matrices by sampling a subset of them. This idea leads to Algorithm 2.1, which approximately solves the training problem and can train ANNs with widths much less than m^* . Algorithm 2.1 is an instance of the approximation described in [45, Remark 3.3], but [45] did not provide theoretical insights regarding its level of suboptimality. The following theorem bridges the gap by providing a probabilistic bound

on the suboptimality of the ANN trained with [Algorithm 2.1](#). The following theorem provides a probabilistic bound on the level of suboptimality of the ANN trained using [Algorithm 2.1](#).

Theorem 2.2. *Consider an additional diagonal matrix D_{P_s+1} sampled uniformly, and construct*

$$(2.6) \quad p_{s2}^* = \min_{(v_h, w_h)_{h=1}^{P_s+1}} \ell \left(\sum_{h=1}^{P_s+1} D_h X(v_h - w_h), y \right) + \beta \sum_{h=1}^{P_s+1} (\|v_h\|_2 + \|w_h\|_2)$$

s. t. $(2D_h - I_n)Xv_h \geq 0, (2D_h - I_n)Xw_h \geq 0, \forall h \in [P_s + 1].$

It holds that $p_{s2}^ \leq p_{s1}^*$. Furthermore, if $P_s \geq \min \left\{ \frac{n+1}{\psi\xi} - 1, \frac{2}{\xi}(n+1 - \log \psi) \right\}$, where ψ and ξ are preset confidence level constants between 0 and 1, then with probability at least $1 - \xi$, it holds that $\mathbb{P}\{p_{s2}^* < p_{s1}^*\} \leq \psi$.*

The proof of [Theorem 2.2](#) is presented in [Appendix E.1](#). Intuitively, [Theorem 2.2](#) shows that sampling an additional D_{P_s+1} matrix will not reduce the training loss with high probability when P_s is large. One can recursively apply this bound T times to show that the solution with P_s matrices is close to the solution with $P_s + T$ matrices for an arbitrary number T . Thus, while the theorem does not directly bound the gap between the approximated optimization problem and its exact counterpart, it states that the optimality gap due to sampling is not too large for a suitable value of P_s , and the trained ANN is nearly optimal.

Compared with the exponential relationship between P and r , a satisfactory value of P_s is linear in n and is independent from r . Thus, when r is large, solving the approximated formulation [\(2.5\)](#) is significantly (exponentially) more efficient than solving the exact formulation [\(2.2\)](#). On the other hand, [Algorithm 2.1](#) is no longer deterministic due to the stochastic sampling of the D_h matrices, and yields solutions that upper-bound those of [\(2.2\)](#).

Since the confidence constants ψ and ξ are no greater than one, [Theorem 2.2](#) only applies to overparameterized ANNs, where $P_s \geq n$. Although [\[45\]](#) has shown that there exists a globally optimal neural network whose width is at most $n + 1$ and [Theorem 2.2](#) seems loose by this comparison, our theorem bounds a different quantity and is meaningful. Specifically, the bound in [\[45\]](#) does not provide a method that scales linearly: while a globally optimal neural network narrower than $n + 1$ exists, finding such an ANN requires solving a convex program with an exponential number of constraints. In contrast, [Theorem 2.2](#) characterizes the optimality of a convex optimization with a manageable number of constraints. In practice, selecting P_s is equivalent to choosing the ANN width. While [Theorem 2.2](#) provides a guideline on how P_s should scale with n , selecting a much smaller P_s will not necessarily become an issue. Our experiments in [subsection 5.1](#) show that even when P_s is much less than n (which is much less than P), [Algorithm 2.1](#) still reliably trains high-performance classifiers.

3. An ADMM Algorithm for Global ANN Training. The convex ReLU ANN training program [\(2.2\)](#) may be solved with the interior point method (IPM). The IPM is an iterative algorithm that repeatedly performs Newton updates. Each Newton update requires solving a linear system, which has a cubic complexity, hindering the application of IPM to large-scale optimization problems. Unfortunately, large-scale problems are ubiquitous in the field of machine learning. This section proposes an algorithm based on the ADMM, breaking down the

optimization problem (2.2) to smaller subproblems that are easier to solve. Moreover, when $\ell(\cdot)$ is the squared loss, each subproblem has a closed-form solution. We will show that the complexity of each ADMM iteration is linear in n and quadratic in d and P , and the number of required ADMM steps to reach a desired precision is logarithmic in the precision level. When other convex loss functions are used, a closed-form solution may not always exist. We illustrate that iterative methods can solve the subproblems for general convex losses efficiently.

Define $F_i := D_i X$ and $G_i := (2D_i - I_n)X$ for all $i \in [P]$. Furthermore, we introduce v_i, w_i, s_i, t_i as slack variables and let $v_i = u_i, w_i = z_i, s_i = G_i v_i$, and $t_i = G_i w_i$. For a vector $q = (q_1, \dots, q_n) \in \mathbb{R}^n$, let the indicator function of the positive quadrant $\mathbb{I}_{\geq 0}$ be defined as

$$\mathbb{I}_{\geq 0}(q) := \begin{cases} 0 & \text{if } q_i \geq 0, \forall i \in [N]; \\ +\infty & \text{otherwise.} \end{cases}$$

The convex training formulation (2.2) can be reformulated as a convex optimization problem with positive quadrant indicator functions and linear equality constraints:

$$(3.1) \quad \begin{aligned} \min_{(v_i, w_i, s_i, t_i, u_i, z_i)_{i=1}^P} & \ell\left(\sum_{i=1}^P F_i(u_i - z_i), y\right) + \beta \sum_{i=1}^P \|v_i\|_2 + \beta \sum_{i=1}^P \|w_i\|_2 + \sum_{i=1}^P \mathbb{I}_{\geq 0}(s_i) + \sum_{i=1}^P \mathbb{I}_{\geq 0}(t_i) \\ \text{s. t.} & \quad G_i u_i - s_i = 0, \quad G_i z_i - t_i = 0, \quad v_i - u_i = 0, \quad w_i - z_i = 0, \quad \forall i \in [P]. \end{aligned}$$

Next, we simplify the notations by concatenating the matrices. Define

$$\begin{aligned} u &:= [u_1^\top \cdots u_P^\top \quad z_1^\top \cdots z_P^\top]^\top, \quad v := [v_1^\top \cdots v_P^\top \quad w_1^\top \cdots w_P^\top]^\top, \\ s &:= [s_1^\top \cdots s_P^\top \quad t_1^\top \cdots t_P^\top]^\top, \\ F &:= [F_1 \cdots F_P \quad -F_1 \cdots -F_P], \quad \text{and } G := \text{blkdiag}(G_1, \dots, G_P, G_1, \dots, G_P), \end{aligned}$$

where $\text{blkdiag}(\cdot, \dots, \cdot)$ denotes the block diagonal matrix formed by the submatrices in the parentheses. The formulation (3.1) is then equivalent to the compact notation

$$(3.2) \quad \min_{v, s, u} \ell(Fu, y) + \beta \|v\|_{2,1} + \mathbb{I}_{\geq 0}(s) \quad \text{s. t.} \quad \begin{bmatrix} I_{2dP} \\ G \end{bmatrix} u - \begin{bmatrix} v \\ s \end{bmatrix} = 0,$$

where $\|\cdot\|_{2,1}$ denotes the ℓ_1 - ℓ_2 mixed norm group sparse regularization and I_{2dP} is the identity matrix in $\mathbb{R}^{2dP \times 2dP}$. The corresponding augmented Lagrangian [29] of (3.2), denoted as $L(u, v, s, \nu, \lambda)$, is:

$$\begin{aligned} L(u, v, s, \nu, \lambda) = & \ell(Fu, y) + \beta \|v\|_{2,1} + \mathbb{I}_{\geq 0}(s) + \frac{\rho}{2} \left(\|u - v + \lambda\|_2^2 - \|\lambda\|_2^2 \right) + \frac{\rho}{2} \left(\|Gu - s + \nu\|_2^2 - \|\nu\|_2^2 \right) \end{aligned}$$

where $\lambda := [\lambda_{11} \cdots \lambda_{1P} \quad \lambda_{21} \cdots \lambda_{2P}]^\top \in \mathbb{R}^{2dP}$ and $\nu := [\nu_{11} \cdots \nu_{1P} \quad \nu_{21} \cdots \nu_{2P}]^\top \in \mathbb{R}^{2nP}$ are dual variables, $\rho > 0$ is a fixed penalty parameter, and $\gamma_a > 0$ is a step-size constant.

Algorithm 3.1 An ADMM algorithm for the convex ANN training problem.

1: **repeat**

2: Primal update

$$(3.3a) \quad u^{k+1} = \arg \min_u \ell(Fu, y) + \frac{\rho}{2} \|u - v^k + \lambda^k\|_2^2 + \frac{\rho}{2} \|Gu - s^k + \nu^k\|_2^2$$

3: Primal update

$$(3.3b) \quad \begin{bmatrix} v^{k+1} \\ s^{k+1} \end{bmatrix} = \arg \min_{v, s} \beta \|v\|_{2,1} + \mathbb{I}_{\geq 0}(s) + \frac{\rho}{2} \|u^{k+1} - v + \lambda^k\|_2^2 + \frac{\rho}{2} \|Gu^{k+1} - s + \nu^k\|_2^2$$

4: Dual update:

$$(3.3c) \quad \begin{bmatrix} \lambda^{k+1} \\ \nu^{k+1} \end{bmatrix} = \begin{bmatrix} \lambda^k + \frac{\gamma_a}{\rho} (u^{k+1} - v^{k+1}) \\ \nu^k + \frac{\gamma_a}{\rho} (Gu^{k+1} - s^{k+1}) \end{bmatrix}$$

5: **end repeat**

We can apply the ADMM iterations described in [Algorithm 3.1](#) to globally optimize [\(3.2\)](#).¹ As will be shown next, [\(3.3b\)](#) and [\(3.3c\)](#) have simple closed-form solutions. The update [\(3.3a\)](#) has a closed-form solution when $\ell(\cdot)$ is the squared loss, and can be efficiently solved numerically for general convex loss functions. When we apply ADMM to solve the approximated convex training formulation [\(2.5\)](#), [Algorithm 3.1](#) becomes a subalgorithm of [Algorithm 2.1](#).

The following theorem shows the linear convergence of the ADMM algorithm, with the proof provided in [Appendix E.2](#):

Theorem 3.1. *If $\ell(\hat{y}, y)$ is strictly convex and continuously differentiable with a uniform Lipschitz continuous gradient with respect to \hat{y} , then the sequence $\{(u^k, v^k, s^k, \lambda^k, \nu^k)\}$ generated by [Algorithm 3.1](#) converges linearly to an optimal primal-dual solution for [\(3.2\)](#), provided that the step size γ_a is sufficiently small.*

Many popular loss functions satisfy the conditions of [Theorem 3.1](#). Examples include the squared loss (for regression) and the binary cross-entropy loss coupled with the tanh or the sigmoid output activation (for binary classification).

3.1. s and v updates. The update step [\(3.3b\)](#) can be separated for v^{k+1} and s^{k+1} as:

$$(3.4a) \quad v^{k+1} = \arg \min_v \beta \|v\|_{2,1} + \frac{\rho}{2} \|u^{k+1} - v + \lambda^k\|_2^2;$$

$$(3.4b) \quad s^{k+1} = \arg \min_{s \geq 0} \mathbb{I}_{\geq 0}(s) + \|Gu^{k+1} - s + \nu^k\|_2^2 = \arg \min_{s \geq 0} \|Gu^{k+1} - s + \nu^k\|_2^2.$$

Note that [\(3.4a\)](#) can be separated for each v_i and w_i (allowing parallelization) and solved analytically using the formulas:

$$v_i^{k+1} = \arg \min_v \beta \|v_i\|_2 + \frac{\rho}{2} \|u_i^{k+1} - v + \lambda_{1i}^k\|_2^2 = \text{prox}_{\frac{\beta}{\rho} \|\cdot\|_2} (u_i^{k+1} + \lambda_{1i}^k)$$

¹The ADMM algorithm is presented in the scaled dual form [\[13\]](#).

$$\begin{aligned}
&= \left(1 - \frac{\beta}{\rho \cdot \|u_i^{k+1} + \lambda_{1i}^k\|_2}\right)_+ (u_i^{k+1} + \lambda_{1i}^k), \quad \forall i \in [P], \\
w_i^{k+1} &= \arg \min_v \beta \|w_i\|_2 + \frac{\rho}{2} \|s_i^{k+1} - w + \lambda_{2i}^k\|_2^2 = \mathbf{prox}_{\frac{\beta}{\rho} \|\cdot\|_2} (z_i^{k+1} + \lambda_{2i}^k) \\
&= \left(1 - \frac{\beta}{\rho \cdot \|z_i^{k+1} + \lambda_{2i}^k\|_2}\right)_+ (z_i^{k+1} + \lambda_{2i}^k), \quad \forall i \in [P],
\end{aligned}$$

where $\mathbf{prox}_{\frac{\beta}{\rho} \|\cdot\|_2}$ denotes the proximal operation on the function $f(\cdot) = \frac{\beta}{\rho} \|\cdot\|_2$. The computational complexity of finding v_i and w_i is $\mathcal{O}(d)$. Similarly, (3.4b) can also be separated for each s_i and t_i and solved analytically using the formulas:

$$\begin{aligned}
s_i^{k+1} &= \arg \min_{s_i \geq 0} \|G_i u_i^{k+1} - s_i + \nu_{1i}^k\|_2^2 = \Pi_{\geq 0}(G_i u_i^{k+1} + \nu_{1i}^k) = (G_i u_i^{k+1} + \nu_{1i}^k)_+, \quad \forall i \in [P]; \\
t_i^{k+1} &= \arg \min_{t_i \geq 0} \|G_i z_i^{k+1} - s_i + \nu_{2i}^k\|_2^2 = \Pi_{\geq 0}(G_i z_i^{k+1} + \nu_{2i}^k) = (G_i z_i^{k+1} + \nu_{2i}^k)_+, \quad \forall i \in [P].
\end{aligned}$$

where $\Pi_{\geq 0}$ denotes the projection onto the non-negative quadrant. The computational complexity of finding s_i and t_i is $\mathcal{O}(n)$. The updates (3.4a) and (3.4b) can be performed in $\mathcal{O}(nP + dP)$ time in total.

3.2. u updates. The u update step depends on the specific structure of $\ell(\cdot)$. For the squared loss, the u update step can be solved in closed form. For many other loss functions, the update can be performed with numerical methods.

3.2.1. Squared loss. The squared loss $\ell(\hat{y}, y) = \frac{1}{2} \|\hat{y} - y\|_2^2$ is a commonly used loss function in machine learning. It is widely used for regression tasks, but can also be used for classification. For the squared loss, (3.3a) amounts to

$$(3.5) \quad u^{k+1} = \arg \min_u \left\{ \|Fu - y\|_2^2 + \frac{\rho}{2} \|u - v^k + \lambda^k\|_2^2 + \frac{\rho}{2} \|Gu - s^k + \nu^k\|_2^2 \right\}.$$

Setting the gradient with respect to u to zero yields that

$$(3.6) \quad \left(I + \frac{1}{\rho} F^\top F + G^\top G\right) u^{k+1} = \frac{1}{\rho} F^\top y + v^k - \lambda^k + G^\top s^k - G^\top \nu^k.$$

Therefore, the u update can be performed by solving the linear system (3.6) in each iteration. While solving a linear system $Ax = b$ for a square matrix A has a cubic time complexity in general, by taking advantage of the structure of (3.6), a quadratic per-iteration complexity can be achieved. Specifically, the matrix $I + \frac{1}{\rho} F^\top F + G^\top G$ is symmetric, positive definite, and fixed throughout the ADMM iterations. In general, solving $Ax = b$ for some symmetric $A \in \mathbb{S}^{2dP \times 2dP}$, $A \succ 0$ and $b \in \mathbb{R}^{2dP}$ can be done via the procedure:

1. Perform the Cholesky decomposition $A = LL^\top$, where L is lower-triangular (cubic in $2dP$);
2. Solve $L\hat{b} = b$ by forward substitution (quadratic in $2dP$);

3. Solve $L^\top x = \hat{b}$ by back substitution (quadratic in $2dP$).

Throughout the ADMM iterations, the first step only needs to be performed once, while the second and the third steps are required for every iteration. Since the dimension of the matrix $(I + \frac{1}{\rho}F^\top F + G^\top G)$ is $2dP \times 2dP$, the per-iteration time complexity of the u update is $\mathcal{O}(d^2P^2)$, making it the most time-consuming step of the ADMM algorithm when d and P are large. Therefore, the overall complexity of a full ADMM primal-dual iteration for the case of squared loss is $\mathcal{O}(nP + d^2P^2)$, which is quadratic. In contrast, the linear system for IPM's Newton updates can be different for each iteration, and thus each iteration has a cubic complexity. Therefore, the proposed ADMM method achieves a notable speed improvement over IPM.

In the case when the approximated formulation (2.5) is considered and P_s diagonal matrices are sampled in place of the full set of P matrices, obtaining a given level of optimality requires P_s to be linear in n , as discussed in section 2. Coupling with the above analysis, we obtain an overall per-iteration complexity of $\mathcal{O}(d^2n^2)$, a significant improvement compared with the $\mathcal{O}(d^3r^3(\frac{n}{r})^{3r})$ per-iteration complexity of [45]. The total computational complexity for reaching a point u^k satisfying $\|u^k - u^*\|_2 \leq \epsilon_a$ is $\mathcal{O}(d^2n^2 \log(1/\epsilon_a))$, where u^* is an optimal value of u and $\epsilon_a > 0$ is a predefined precision threshold. In subsection 5.2, we use numerical experiments to demonstrate that the improved efficiency of the ADMM algorithm enables the application of convex ANN training to image classification tasks, which was not possible before. Moreover, our experiments show that a favorable prediction accuracy may only require a moderate optimization precision, which can be reached with a few ADMM iterations.

3.2.2. General convex loss functions. When a general convex loss function $\ell(\hat{y}, y)$ is considered, a closed-form solution to (3.3a) does not always exist and one may need to use iterative methods to solve (3.3a). One natural use of an iterative optimization method is gradient descent. However, for large-scale problems, a full gradient evaluation can be too expensive. To address this issue, we exploit the symmetric and separable property of each u_i and z_i in (3.3a) and propose an application of the randomized block coordinate descent (RBCD) method. The details of RBCD are presented in Algorithm 3.2. The superscript $+$ denotes the updated quantities for each iteration, and the notation γ_r is the step size. In practice, the RBCD step size γ_r can be adaptively chosen with a backtracking line search. Steps 5 and 6 of Algorithm 3.2 are derived via the chain rule of differentiation. It can be verified that (3.3a) is always strongly convex because its second term is strongly convex while the first and third terms are convex. [41, Theorem 1] has shown that when minimizing strongly-convex functions, RBCD converges linearly. The theoretical convergence rate is higher when the convexity of (3.3a) is stronger and P is smaller.

Furthermore, $G_i^\top G_i = X^\top X$ for all $i \in [P]$. To see this, recall that $G_i = (2D_i - I_n)X$ by definition. Since $(2D_i - I_n)$ is a diagonal matrix with all entries being ± 1 , it holds that $(2D_i - I_n)^\top (2D_i - I_n) = I_n$. Thus, $G_i^\top G_i = X^\top (2D_i - I_n)^\top (2D_i - I_n) X = X^\top X$. Consequently, $X^\top X$ can be assembled in advance, and there is no need to compute $G_i^\top G_i$ in each iteration. The most expensive calculations per RBCD update thus have the following complexities:

Algorithm 3.2 Randomized Block Coordinate Descent (RBCD)

-
- 1: Initialize $\hat{y} = \sum_{i=1}^P F_i(u_i - z_i)$;
 - 2: Fix $\tilde{s}_i = G_i^\top (s_i - \nu_{1i})$, $\tilde{t}_i = G_i^\top (t_i - \nu_{2i})$ for all $i \in [P]$;
 - 3: Select accuracy thresholds $\tau > 0, \varphi > 0$;
 - 4: **repeat**
 - 5: $\tilde{y} \leftarrow \nabla_{\hat{y}} \ell(\hat{y}, y)$
 - 6: Uniformly select i from $[P]$ at random;
 - 7: $u_i^+ \leftarrow u_i - \gamma_r F_i^\top \tilde{y} - \gamma_r \rho(u_i - v_i + \lambda_{1i} + G_i^\top G_i u_i - \tilde{s}_i)$;
 - 8: $z_i^+ \leftarrow z_i + \gamma_r F_i^\top \tilde{y} - \gamma_r \rho(z_i - w_i + \lambda_{2i} + G_i^\top G_i z_i - \tilde{t}_i)$;
 - 9: $\hat{y}^+ \leftarrow \hat{y} + F_i((u_i^+ - z_i^+) - (u_i + z_i))$;
 - 10: **until** $\|\nabla_u L(u, v, s, \nu, \lambda)\|_2 \leq \frac{\varphi}{\max\{\tau, \|u\|_2\}}$.
-

$$\frac{F_i^\top \tilde{y} \quad \left| \quad F_i((u_i^+ - z_i^+) - (u_i + z_i)) \quad \left| \quad (X^\top X)u_i \quad \left| \quad (X^\top X)z_i \quad \right. \right.}{\mathcal{O}(nd) \quad \left| \quad \mathcal{O}(nd) \quad \left| \quad \mathcal{O}(d^2) \quad \left| \quad \mathcal{O}(d^2). \quad \right. \right.}$$

While it can be costly to solve (3.3a) to a high accuracy using iterative methods, especially during the early iterations of ADMM, [22, Algorithm 1, Prop 6] has shown that even when (3.3a) is solved approximately, as long as the accuracy threshold φ of each ADMM iteration forms a convergent sequence, the ADMM algorithm can eventually converge to the global optimum of (3.2). Each iterative solution of the u -update subproblem can also take advantage of warm-starting by initializing at the result of the previous ADMM iteration. As a result, we alternate between an ADMM update and several RBCD updates in a delicate manner.

4. Convex Adversarial Training. The inherent difficulties with adversarial training can be addressed by taking advantage of the convex training framework and the related algorithms.

4.1. Background about adversarial training. A classifier is considered robust against adversarial perturbations if it assigns the same label to all inputs within an ℓ_∞ bound with radius ϵ [26]. The perturbation set can then be defined as

$$\mathcal{X} = \left\{ X + \Delta \in \mathbb{R}^{n \times d} \mid \Delta = [\delta_1, \dots, \delta_n]^\top, \delta_k \in \mathbb{R}^d, \|\delta_k\|_\infty \leq \epsilon, \forall k \in [n] \right\}.$$

In this work, we consider the “white box” setting, where the adversary has complete knowledge about the ANN. One common method for training robust classifiers is to minimize the maximum loss within the perturbation set by solving the following minimax problem: [43]

$$(4.1) \quad \min_{(u_j, \alpha_j)_{j=1}^m} \left(\max_{\Delta: X+\Delta \in \mathcal{X}} \ell \left(\sum_{j=1}^m ((X + \Delta)u_j)_+ \alpha_j, y \right) + \frac{\beta}{2} \sum_{j=1}^m (\|u_j\|_2^2 + \alpha_j^2) \right).$$

This process of “training with adversarial data” is often referred to as “adversarial training”, as opposed to “standard training” that trains on clean data. In the prior literature, Fast

Gradient Sign Method (FGSM) and Projected Gradient Descent (PGD) are commonly used to numerically solve the inner maximization of (4.1) and generate adversarial examples in practice [43]. More specifically, FGSM generates adversarial examples \tilde{x} using

$$(4.2) \quad \tilde{x} = x + \epsilon \cdot \text{sgn}\left(\nabla_x \ell\left(\sum_{j=1}^m (x^\top u_j)_+ \alpha_j, y\right)\right).$$

Since FGSM is a one-shot method that assumes linearity, it may miss the worst-case adversarial input. PGD better explores the nonlinear landscape of the problem and is capable of generating “universal” first-order adversaries by running the iterations

$$(4.3) \quad \tilde{x}^{t+1} = \Pi_{\mathcal{X}}\left(\tilde{x}^t + \gamma_p \cdot \text{sgn}\left(\nabla_x \ell\left(\sum_{j=1}^m (x^\top u_j)_+ \alpha_j, y\right)\right)\right)$$

for $t = 0, 1, \dots$, where x^t is the perturbed data vector at the t^{th} iteration and $\gamma_p > 0$ is the step size. The initial vector \tilde{x}^0 is the unperturbed data x .

4.2. The convex adversarial training formulation. While PGD adversaries have been considered “universal” in the literature, adversarial training with PGD adversaries has several limitations. Since the optimization landscapes are generally non-concave over the perturbation Δ , there is no guarantee that PGD will find the true worst-case adversary. Furthermore, traditional adversarial training solves complicated bi-level minimax optimization problems, exacerbating the instability of non-convex ANN training. Our experiments show that back-propagation gradient methods can struggle to converge when solving (4.1). Moreover, solving the bi-level optimization (4.1) requires an algorithm with a computationally cumbersome nested loop structure. To conquer such difficulties, we leverage [Theorem 2.1](#) to re-characterize (4.1) as robust, convex upper-bound problems that can be efficiently solved globally.

We first develop a result about adversarial training involving general convex loss functions. The connection between the convex training objective and the non-convex ANN loss function holds only when the linear constraints in (2.2) are satisfied. For adversarial training, we need this connection to hold at all perturbed data matrices $X + \Delta \in \mathcal{X}$. Otherwise, if some matrix $X + \Delta$ violates the linear constraints, then this perturbation Δ can correspond to a low convex objective value but a high actual loss. To ensure the correctness of the convex reformulation throughout \mathcal{X} , we introduce some robust constraints below.

Since the D_i matrices in (2.2) reflects the ReLU patterns of X , these matrices can change when X is perturbed. Therefore, we include all distinct diagonal matrices $\text{diag}([(X + \Delta)u \geq 0])$ that can be obtained for all $u \in \mathbb{R}^d$ and all $\Delta : X + \Delta \in \mathcal{U}$, denoted as $D_1, \dots, D_{\hat{P}}$, where \hat{P} is the total number of such matrices. Since $D_1, \dots, D_{\hat{P}}$ include D_1, \dots, D_P in (2.2), we have $\hat{P} \geq P$. While \hat{P} is at most 2^n in the worst case, since ϵ is often small, we expect \hat{P} to be relatively close to P , where $P \leq 2r \left(\frac{e(n-1)}{r}\right)^r$ as discussed above.

Finally, we replace the objective of the convex standard training formulation (2.2) with its

robust counterpart, giving rise to the optimization

$$(5.4a) \quad \min_{(v_i, w_i)_{i=1}^{\hat{P}}} \left(\max_{\Delta: X+\Delta \in \mathcal{U}} \ell \left(\sum_{i=1}^{\hat{P}} D_i(X+\Delta)(v_i - w_i), y \right) + \beta \sum_{i=1}^{\hat{P}} (\|v_i\|_2 + \|w_i\|_2) \right)$$

$$(5.4b) \quad \text{s. t.} \quad \min_{\Delta: X+\Delta \in \mathcal{U}} (2D_i - I_n)(X+\Delta)v_i \geq 0, \quad \min_{\Delta: X+\Delta \in \mathcal{U}} (2D_i - I_n)(X+\Delta)w_i \geq 0, \quad \forall i \in [\hat{P}]$$

where \mathcal{U} is any convex additive perturbation set. The next theorem shows that (4.4) is an upper-bound to the robust loss function (4.1), with the proof provided in Appendix E.5.

Theorem 4.1. *Let $(v_{rob_i}^*, w_{rob_i}^*)_{i=1}^{\hat{P}}$ denote a solution of (4.4) and define \hat{m}^* as $|\{i : v_{rob_i}^* \neq 0\}| + |\{i : w_{rob_i}^* \neq 0\}|$. When the ANN width m satisfies $m \geq \hat{m}^*$, the optimization problem (4.4) provides an upper-bound on the non-convex adversarial training problem (4.1). The robust ANN weights $(u_{rob_j}^*, \alpha_{rob_j}^*)_{j=1}^{\hat{m}^*}$ can be recovered using (2.4).*

When the perturbation set is zero, Theorem 4.1 reduces to Theorem 2.1. In light of Theorem 4.1, we use optimization (4.4) as a surrogate for the optimization (4.1) to train the ANN. Since (4.4) includes all D_i matrices in (2.2), we have $\hat{P} \geq P$. While \hat{P} is at most 2^n in the worst case, since ϵ is often small, we expect \hat{P} to be relatively close to P , where $P \leq 2r \left(\frac{e(n-1)}{r} \right)^r$ as discussed above. As will be shown in subsection 4.3, an approximation to (4.4) can be applied to train ANNs with width much less than \hat{m}^* .

The robust constraints in (5.4b) force all points within the perturbation set to be feasible. Intuitively, for every $j \in [\hat{m}^*]$, (5.4b) forces the ReLU activation pattern $\text{sgn}((X+\Delta)u_{rob_j}^*)$ to stay the same for all Δ such that $X+\Delta \in \mathcal{U}$. Moreover, if Δ_{rob}^* denotes a solution to the inner maximization in (5.4a), then $X+\Delta_{rob}^*$ corresponds to the worst-case adversarial inputs for the recovered ANN.

Corollary 4.2. *For the perturbation set \mathcal{X} , the constraints in (5.4b) are equivalent to*

$$(4.5) \quad (2D_i - I_n)Xv_i \geq \epsilon \|v_i\|_1, \quad (2D_i - I_n)Xw_i \geq \epsilon \|w_i\|_1, \quad \forall i \in [\hat{P}].$$

The proof of Corollary 4.2 is provided in Appendix E.6. Note that the left side of each inequality in (4.5) is a vector while the right side is a scalar, which means that each element of the corresponding vector should be greater than or equal to that scalar.

We will show that the new problem can be efficiently solved in important cases. Specifically, (4.4) reduces to a classic convex optimization problem when $\ell(\hat{y}, y)$ is the hinge loss, the squared loss, or the binary cross-entropy loss. Due to space restrictions, the result for the squared loss is presented in Appendix D.1.

4.3. Practical algorithm for convex adversarial training. Since Theorem 2.2 does not rely on assumptions about the matrix X , it applies to an arbitrary $X+\Delta$ matrix, and naturally extends to the convex adversarial training formulation (4.4). Therefore, an approximation to (4.4) can be applied to train robust ANNs with widths much less than \hat{m}^* . Similar to the strategy rendered in Algorithm 2.1, we use a subset of the D_i matrices for practical adversarial

Algorithm 4.1 Practical convex adversarial training

-
- 1: **for** $h = 1$ to P_a **do**
 - 2: $a_h \sim \mathcal{N}(0, I_d)$ i.i.d.
 - 3: $D_{h1} \leftarrow \text{diag}([Xa_h \geq 0])$
 - 4: **for** $j = 2$ to S **do**
 - 5: $R_{hj} \leftarrow [r_1, \dots, r_d]$, where $r_\kappa \sim \mathcal{N}(\mathbf{0}, I_n), \forall \kappa \in [d]$
 - 6: $D_{hj} \leftarrow \text{diag}([\bar{X}_{hj}a_h \geq 0])$, where $\bar{X}_{hj} \leftarrow X + \epsilon \cdot \text{sgn}(R_{hj})$
 - 7: Discard repeated D_{hj} matrices
 - 8: **break if** P_s distinct D_{hj} matrices has been generated
 - 9: **end for**
 - 10: **end for**
 - 11: Solve

$$(4.6) \quad \min_{(v_i, w_i)_{i=1}^{\bar{P}}} \left(\max_{\Delta: X+\Delta \in \mathcal{U}} \ell \left(\sum_{h=1}^{P_s} D_h(X+\Delta)(v_h - w_h), y \right) + \beta \sum_{h=1}^{P_s} (\|v_h\|_2 + \|w_h\|_2) \right)$$

s. t. $\min_{\Delta: X+\Delta \in \mathcal{U}} (2D_h - I_n)(X+\Delta)v_h \geq 0, \quad \forall h \in [P_s],$
 $\min_{\Delta: X+\Delta \in \mathcal{U}} (2D_h - I_n)(X+\Delta)w_h \geq 0, \quad \forall h \in [P_s].$
 - 12: Recover u_1, \dots, u_{m_s} and $\alpha_1, \dots, \alpha_{m_s}$ from the solution $(v_{\text{robs}_h}^*, w_{\text{robs}_h}^*)_{h=1}^{P_s}$ of (4.6) using (2.4).
-

training. Since the D_i matrices depend on the perturbation Δ , we also add randomness to the data matrix X in the sampling process to cover D_i matrices associated with different perturbations, leading to Algorithm 4.1. P_a and S are preset parameters that determine the number of random weight samples, with $P_a \times S \geq P_s$.

4.4. Convex hinge loss adversarial training. While the inner maximization of the robust problem (4.4) is still hard to solve in general, it is tractable for some loss functions. The simplest case is the piecewise-linear hinge loss $\ell(\hat{y}, y) = (1 - \hat{y} \odot y)_+$, which is widely used for classification. Here, we focus on binary classification with $y \in \{-1, 1\}^n$.²

Consider the training problem for a one-hidden-layer ANN with ℓ_2 regularized hinge loss:

$$(4.7) \quad \min_{(u_j, \alpha_j)_{j=1}^m} \left(\frac{1}{n} \cdot \mathbf{1}^\top \left(\mathbf{1} - y \odot \sum_{j=1}^m (Xu_j)_+ \alpha_j \right)_+ + \frac{\beta}{2} \sum_{j=1}^m (\|u_j\|_2^2 + \alpha_j^2) \right)$$

The adversarial training problem considering the ℓ_∞ -bounded adversarial data perturbation set \mathcal{X} is:

$$(4.8) \quad \min_{(u_j, \alpha_j)_{j=1}^m} \left(\max_{\Delta: X+\Delta \in \mathcal{X}} \frac{1}{n} \cdot \mathbf{1}^\top \left(\mathbf{1} - y \odot \sum_{j=1}^m ((X+\Delta)u_j)_+ \alpha_j \right)_+ + \frac{\beta}{2} \sum_{j=1}^m (\|u_j\|_2^2 + \alpha_j^2) \right)$$

²Other ℓ_p norm-bounded additive perturbation sets can be similarly analyzed, as shown in Appendix D.3. It is also straightforward to extend the analysis in this section to any convex piecewise-affine loss functions.

Applying [Theorem 4.1](#) and [Corollary 4.2](#) leads to the following formulation as an upper bound on [\(4.8\)](#):

$$(4.9) \quad \min_{(v_i, w_i)_{i=1}^{\hat{P}}} \left(\max_{\Delta: X+\Delta \in \mathcal{X}} \frac{1}{n} \cdot \mathbf{1}^\top \left(\mathbf{1} - y \odot \sum_{i=1}^{\hat{P}} D_i(X + \Delta)(v_i - w_i) \right)_+ + \beta \sum_{i=1}^{\hat{P}} (\|v_i\|_2 + \|w_i\|_2) \right)$$

s. t. $(2D_i - I_n)Xv_i \geq \epsilon\|v_i\|_1, (2D_i - I_n)Xw_i \geq \epsilon\|w_i\|_1, \forall i \in [\hat{P}].$

For the purpose of generating the $D_1, \dots, D_{\hat{P}}$ matrices, instead of enumerating an infinite number of points in \mathcal{X} , we only need to enumerate all vertices of \mathcal{X} , which is finite. This is because the solution Δ_{hinge}^* to the inner maximum always occurs at a vertex of \mathcal{X} , as will be shown in [Theorem 4.3](#). Solving the inner maximization of [\(4.9\)](#) in closed form leads to the next theorem, whose proof is provided in [Appendix E.7](#).

Theorem 4.3. *For the binary classification problem, the inner maximum of [\(4.9\)](#) is attained at $\Delta_{\text{hinge}}^* = -\epsilon \cdot \text{sgn}\left(\sum_{i=1}^{\hat{P}} D_i y (v_i - w_i)^\top\right)$, and the bi-level optimization problem [\(4.9\)](#) is equivalent to the classic optimization problem:*

$$(4.10) \quad \min_{(v_i, w_i)_{i=1}^{\hat{P}}} \left(\frac{1}{n} \sum_{k=1}^n \left(1 - y_k \sum_{i=1}^{\hat{P}} d_{ik} x_k^\top (v_i - w_i) + \epsilon \left\| \sum_{i=1}^{\hat{P}} d_{ik} (v_i - w_i) \right\|_1 \right)_+ + \beta \sum_{i=1}^{\hat{P}} (\|v_i\|_2 + \|w_i\|_2) \right)$$

s. t. $(2D_i - I_n)Xv_i \geq \epsilon\|v_i\|_1, (2D_i - I_n)Xw_i \geq \epsilon\|w_i\|_1, \forall i \in [\hat{P}],$

where d_{ik} denotes the k^{th} diagonal element of D_i .

The problem [\(4.10\)](#) is a finite-dimensional convex program that upper-bounds [\(4.8\)](#), the robust counterpart of [\(4.7\)](#). We can thus solve [\(4.10\)](#) to robustly train the ANN.

4.5. Convex binary cross-entropy loss adversarial training. The binary cross-entropy loss is also widely used in binary classification. Here, we consider a scalar-output ANN with a scaled tanh output layer for binary classification with $y \in \{0, 1\}^n$. The loss function $\ell(\cdot)$ in this case is $\ell(\hat{y}, y) = -2\hat{y}^\top y + \mathbf{1}^\top \log(e^{2\hat{y}} + 1)$. The non-convex adversarial training formulation considering the ℓ_∞ -bounded data uncertainty set \mathcal{X} is then:

$$(4.11) \quad \min_{(u_j, \alpha_j)_{j=1}^m} \left(\max_{\|\Delta\|_{\max} \leq \epsilon} \frac{1}{n} \sum_{k=1}^n \left(-2\hat{y}_k y_k + \log(e^{2\hat{y}_k} + 1) \right) \right) + \frac{\beta}{2} \sum_{j=1}^m (\|u_j\|_2^2 + \alpha_j^2)$$

s. t. $\hat{y} = \sum_{j=1}^m ((X + \Delta)u_j)_+ \alpha_j.$

Applying [Theorem 4.1](#) and [Corollary 4.2](#) leads to the following optimization as an upper bound on [\(4.11\)](#):

$$(4.12) \quad \begin{aligned} & \min_{(v_i, w_i)_{i=1}^{\hat{P}}} \left(\max_{\|\Delta\|_{\max} \leq \epsilon} \frac{1}{n} \sum_{k=1}^n \left(-2\hat{y}_k y_k + \log(e^{2\hat{y}_k} + 1) \right) \right) + \beta \sum_{i=1}^{\hat{P}} (\|v_i\|_2 + \|w_i\|_2) \\ & \text{s. t.} \quad (2D_i - I_n)Xv_i \geq \epsilon\|v_i\|_1, \quad (2D_i - I_n)Xw_i \geq \epsilon\|w_i\|_1, \quad \forall i \in [\hat{P}], \\ & \quad \hat{y}_k = \sum_{i=1}^{\hat{P}} d_{ik} x_k^\top (v_i - w_i) + \sum_{i=1}^{\hat{P}} d_{ik} \delta_k^\top (v_i - w_i). \end{aligned}$$

Consider the formulation

$$(4.13) \quad \begin{aligned} & \min_{(v_i, w_i)_{i=1}^{\hat{P}}} \frac{1}{n} \left(\sum_{k=1}^n f \circ g_k(\{v_i, w_i\}_{i=1}^{\hat{P}}) \right) + \beta \sum_{i=1}^{\hat{P}} (\|v_i\|_2 + \|w_i\|_2) \\ & \text{s. t.} \quad (2D_i - I_n)Xv_i \geq \epsilon\|v_i\|_1, \quad (2D_i - I_n)Xw_i \geq \epsilon\|w_i\|_1, \quad \forall i \in [\hat{P}] \\ & f(u) = \log(e^{2u} + 1), \\ & g_k(\{v_i, w_i\}_{i=1}^{\hat{P}}) = (2y_k - 1) \sum_{i=1}^{\hat{P}} d_{ik} x_k^\top (v_i - w_i) + \epsilon \cdot \left\| \sum_{i=1}^{\hat{P}} d_{ik} (v_i - w_i) \right\|_1, \quad \forall k \in [n]. \end{aligned}$$

The next theorem establishes the equivalence between [\(4.13\)](#) and [\(4.12\)](#). The proof is provided in [Appendix E.9](#).

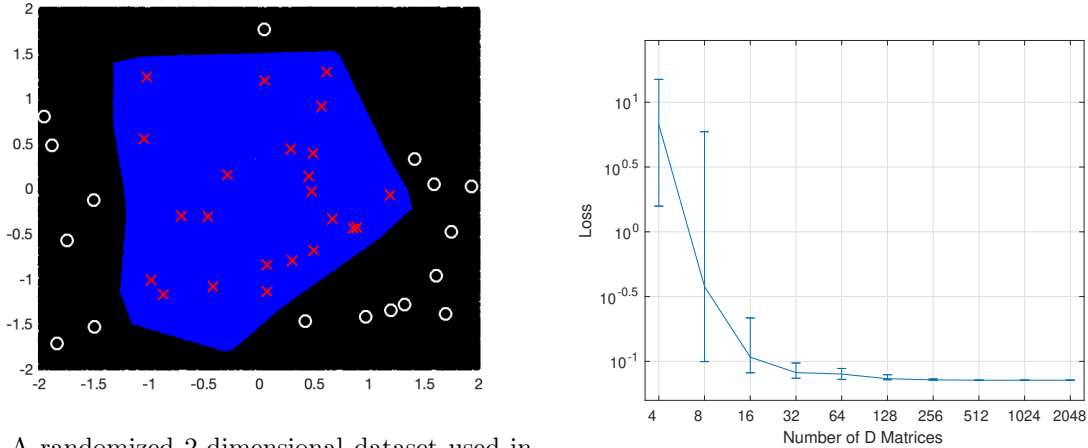
Theorem 4.4. *The optimization [\(4.13\)](#) is a convex program that is equivalent to the bi-level optimization [\(4.12\)](#), and can be used as a surrogate for [\(4.11\)](#) to train robust ANNs. The worst-case perturbation is $\Delta_{BCE}^* = -\epsilon \cdot \text{sgn}\left((2y - 1) \sum_{i=1}^{\hat{P}} D_i (v_i - w_i)^\top\right)$.*

Note that the worst-case perturbation occurs at the same location as for the hinge loss case, which is a vertex in \mathcal{X} . Thus, for the purpose of generating the $D_1, \dots, D_{\hat{P}}$ matrices, we again only need to enumerate all vertices of \mathcal{X} instead of all points in \mathcal{X} .

5. Numerical Experiments.

5.1. Approximated convex standard training. In this subsection, we use numerical experiments to demonstrate the efficacy of practical standard training ([Algorithm 2.1](#)) and to show the level of suboptimality of the ANN trained using [Algorithm 2.1](#).³ The experiment was performed on a randomly-generated dataset with $n = 40$ and $d = 2$ shown in [Figure 1a](#). The upper bound on the number of ReLU activation patterns is $4\left(\frac{e^{(39)}}{2}\right)^2 = 11239$. We ran [Algorithm 2.1](#) to train ANNs using the hinge loss with the number of D_h matrices equal to

³For all experiments in this paper, CVX [\[27\]](#) and CVXPY [\[1, 19\]](#) with the MOSEK [\[5\]](#) solver was used for solving optimization on a laptop computer, unless otherwise stated. Off-the-shelf solvers supported by CVX and CVXPY often treat the convex training problem as a general SOCP. Among all solvers that we experimented on the convex training formulation, MOSEK is the most efficient.



(a) A randomized 2-dimensional dataset used in this experiment. The red crosses are positive training points and the white circles are negative training points. The region classified as positive is in blue, whereas the negative region is in black.

(b) The optimized training loss for each P_s . When P_s reaches 128, the mean and variance of the optimized loss become very small.

Figure 1: Analyzing the effect of P_s on convex standard training.

4, 8, 16, \dots , 2048 and compared the optimized loss.⁴ We repeated this experiment 15 times for each setting, and plotted the loss in Figure 1b. The error bars show the loss values achieved in the best and the worst runs. When there are more than 128 matrices (much less than the theoretical bound on P), Algorithm 2.1 yields consistent and favorable results. Further increasing the number of D matrices does not produce a significantly lower loss. By Theorem 2.2, $P_s = 128$ corresponds to $\psi\xi = 0.318$.

5.2. The ADMM convex training algorithm. We now present the experiment results with the ADMM training algorithm. We use Algorithm 3.1 to solve the approximate convex training formulation (2.5) with the sampled D_h matrices. The hyperparameter settings for the experiments are discussed in Appendix C.1, where we also present guidelines on selecting the ADMM hyperparameters.

5.2.1. Squared loss (closed form u updates) – convergence. For the case of the squared loss, the closed-form solution (3.6) is used for the u updates. We first demonstrate the convergence of the proposed ADMM algorithm using illustrative random data with dimensions $n = 6, d = 5, P_s = 8$. CVX [27] with the IPM-based MOSEK solver [5] was used to solve the optimal objective of (2.2) as the ground truth.

We first explain the notations used in the figures. We use l_{CVX}^* to denote the CVX optimal

⁴To reliably sample P_s matrices, $P_a \cdot S$ in Algorithm 4.1 was set to a large number (81920), and the sampling was terminated when a sufficient number of D_h matrices was generated. The regularization strength β was chosen as 10^{-4} .

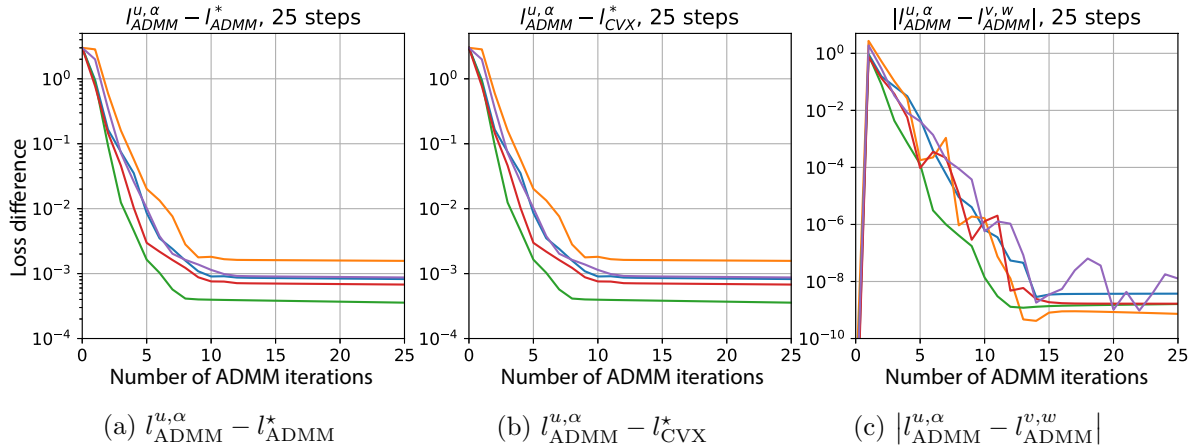


Figure 2: Gap between the cost returned by ADMM for the first 25 iterations and the true optimal cost for the five independent runs.

objective and use l_{ADMM}^* to denote the objective that ADMM converges to as the number of iterations k goes to infinity. There are several methods to calculate the training loss obtained by ADMM. For fair comparisons among ADMM, CVX, and SGD, we use (2.4) to recover the ANN weights $(u_j, \alpha_j)_{j=1}^m$ from the ADMM optimization variables $(v_h^k, w_h^k)_{h=1}^{P_s}$, and use $(u_j, \alpha_j)_{j=1}^m$ to calculate the true non-convex training loss (2.1). The loss at each iteration calculated via this method is denoted as $l_{ADMM}^{u,\alpha}$, and the ADMM solution l_{ADMM}^* is also calculated via this method. At each iteration, we also compute the convex objective of (2.2) using $(v_h^k, w_h^k)_{h=1}^{P_s}$, denoted as $l_{ADMM}^{v,w}$. Since ADMM uses dual variables to enforce the constraints, while the ADMM solution is feasible as k goes to infinity, the intermediate iterations may not be feasible. When the constraints in (2.2) are satisfied, it holds that $l_{ADMM}^{u,\alpha} = l_{ADMM}^{v,w}$. Otherwise, $l_{ADMM}^{u,\alpha}$ may be different from $l_{ADMM}^{v,w}$. The gap between $l_{ADMM}^{u,\alpha}$ and $l_{ADMM}^{v,w}$ indirectly characterizes the feasibility of the ADMM intermediate solutions. When this gap is small, $(v_h^k, w_h^k)_{h=1}^{P_s}$ should be almost feasible. When this gap is large, the constraints may have been severely violated.

While it can be expensive for ADMM to converge to a high precision, an approximate solution is usually sufficient for ANN training. Figure 2a, 2b shows that a precision of 10^{-3} can be achieved within 25 iterations. Moreover, Figure 2c shows that the solution after 25 iterations violates the constraints insignificantly. This behavior of “converging rapidly in the first several steps and slowing down (to a linear rate) afterward” is typical for the ADMM algorithm. As will be shown next, a medium-accuracy solution returned by only a few ADMM iterations can achieve a better prediction performance than the CVX solution. In Appendix B.1, we present empirical results that demonstrate the asymptotic convergence properties of ADMM.

To visualize how the prediction performance achieved by the model changes as the ADMM iteration progresses, we run the ADMM iterations on the “mammographic masses” dataset from the UCI Machine Learning Repository [21], and record the prediction accuracy on the

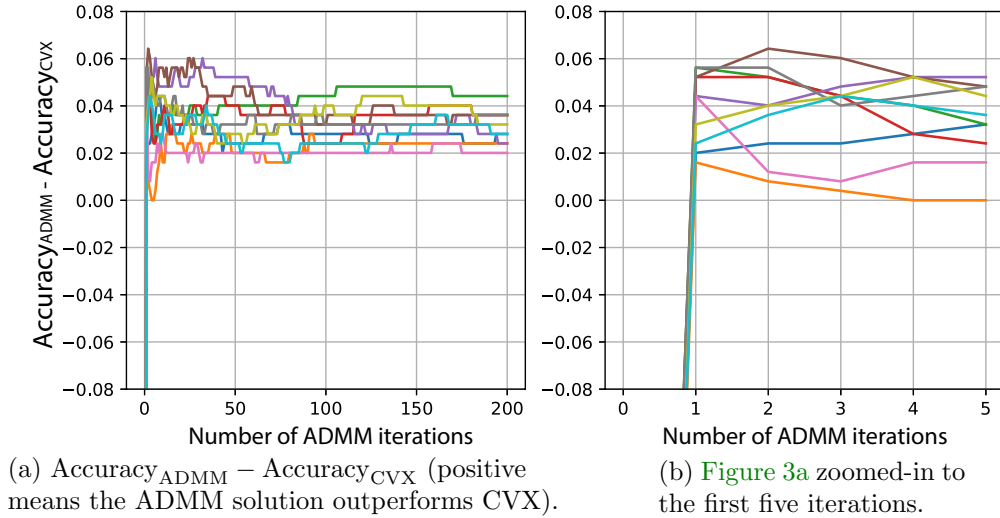


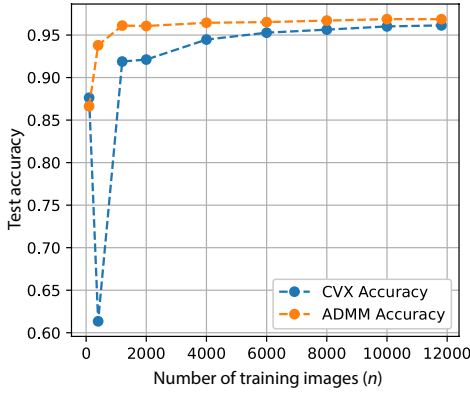
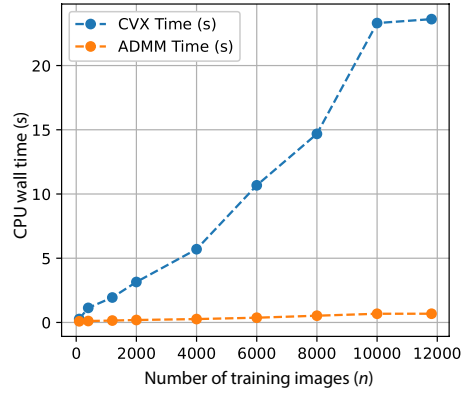
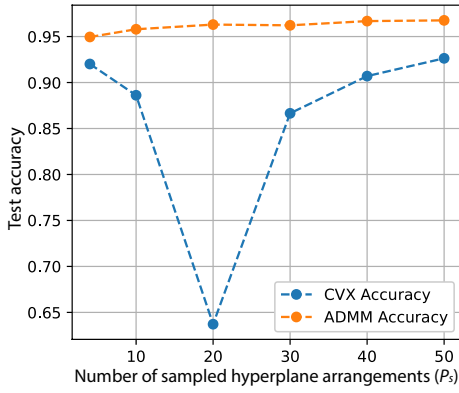
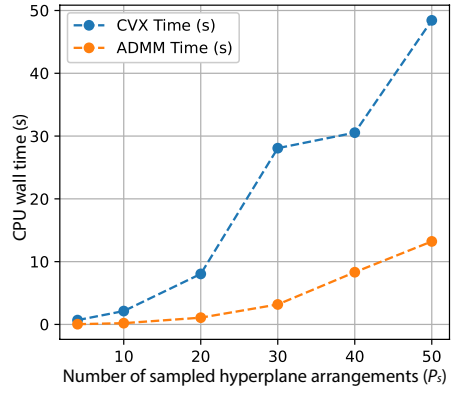
Figure 3: Comparing the ANNs trained with ADMM and with CVX over ten independent runs on the mammographic masses dataset.

test set at each iteration. 70% of the dataset is randomly selected as the training set, and the other 30% is used as the test set. Figure 3 plots the difference between the ADMM accuracies and the CVX accuracies at each iteration.

All ten runs achieves superior test accuracies throughout the first 200 iterations compared with the CVX baseline, and even the first five iterations outperforms the baseline, with the best run outperforming the baseline by 6%. After about 80 iterations, the accuracies stabilize at around 2% to 4% better than the CVX baseline. In conclusion, the prediction performance of the classifiers trained by ADMM is superior even when only a few iterations are run.

5.2.2. Squared loss (closed form u updates) – complexity. To demonstrate the computational complexity of the proposed ADMM method, we used the ADMM method to train ANNs on a downsampled version of the MNIST handwritten digits database with $d = 100$. The task was to perform binary classification between digits “2” and “8”. We first fix $P_s = 8$ and vary n from 100 to 11809.⁵ We independently repeat the experiment five times for each n setting, and present the averaged results in Figure 4a, 4b. In each experiment, ADMM is allowed to run six iterations, which is sufficient to train an accurate ANN. For all choices of n except $n = 100$, the ANNs trained with ADMM attains higher accuracies than CVX networks. This is because while ADMM and CVX solve the same problem, the medium-precision solution from ADMM generalizes better than the high-precision CVX solution. More importantly, as n increases, the CPU time required for CVX grows much faster than ADMM’s execution time, which increases linearly in n . While it is also theoretically possible to run the IPM to a medium precision, even a few IPM iterations become too expensive when n is large. More-

⁵11809 is the total number of 2’s and 8’s in the training set.

(a) Average test accuracy for each n .(b) Average CPU wall time for each n .(c) Average test accuracy for each P_s .(d) Average CPU wall time for each P_s .Figure 4: Analyzing the effect of n and P_s on ADMM convex training with the MNIST dataset.

over, since the IPM uses barrier functions to approximate the constraints, a medium-precision solution produced by the IPM may have feasibility issues, while the ADMM solution sequence generally has good feasibility, as illustrated in Figure 2.

Similarly, we fix $n = 1000$ and vary P_s from 4 to 50. The averaged results over five runs are shown in Figure 4c, 4d. Once again, the proposed ADMM algorithm achieves a higher accuracy for each P_s , and the average CPU time required for ADMM grows much slower than the CVX CPU time. When P_s is 20, all five runs with CVX achieves a low test accuracy, possibly because the structure of the true underlying distribution cannot be well approximated with a linear combination of 20 linear classifiers. Figure 4c, 4d also show that the CPU time scales quadratically with P_s , supporting our analysis of an $\mathcal{O}(nP_s + d^2P_s^2)$ per-iteration complexity.

5.2.3. Squared loss (closed form u updates) – MNIST and Fashion MNIST. Finally, we demonstrate the effectiveness of the proposed ADMM algorithm on all images of “2” and “8” in the MNIST dataset without downsampling ($n = 11809$ and $d = 784$). The parameter

| Method | Test Accuracy | CPU Time (s) | Training Loss | Global Convergence |
|-----------|---------------|--------------|---------------|--------------------|
| Back-prop | 98.86 % | 74.09 | 422.4 | No |
| CVX | 70.99 % | 14879 | 1.146 | Yes |
| ADMM | 98.90 % | 802.2 | 223.2 | Yes |

Table 2: Averaged experiment results with the squared loss on the MNIST dataset over five independent runs. We run 10 ADMM iterations for each setting.

| Method | Test Accuracy | CPU Time (s) | Training Loss | Global Convergence |
|----------------|-----------------|--------------|---------------|--------------------|
| Back-prop | 98.40% (.212%) | 74.09 | 540.0 (40.98) | No |
| ADMM | 98.52% (.0200%) | 423.5 | 119.0 (13.24) | Yes |
| Back-prop (DS) | 98.12% (.157%) | 25.03 | 677.1 (21.20) | No |
| ADMM (DS) | 98.45% (.0912%) | 11.45 | 420.1 (31.50) | Yes |

Table 3: Averaged experiment results with the squared loss on the Fashion MNIST dataset over five independent runs. We run 30 ADMM iterations for each setting. “DS” denotes downsampling. The numbers in the parentheses are the standard deviations over the five runs.

P_s was chosen to be 24, corresponding to a network width of at most 48. The prediction accuracy on the test set, the training loss, and the CPU time are shown in Table 2. The baseline method “CVX” corresponds to using CVX to globally optimize the ANN by solving (2.2), while “Back-prop” denotes the conventional method that performs a SGD local search on the non-convex cost function (2.1).

Table 2 shows that ADMM achieves a higher test accuracy than both CVX and back-propagation SGD. Once again, while ADMM and CVX solve the same problem and CVX achieves a lower loss, the CVX solution suffers from overfitting and thus cannot generalize well to the test data. The training loss returned by ADMM is higher than the true optimal cost but lower than the back-propagation solution. The training time of ADMM is considerably shorter than CVX. Specifically, assembling the matrix $I + \frac{1}{\rho}F^\top F + G^\top G$ required 22% of the time, and the Cholesky decomposition needed 34% of the time, while each ADMM iteration only took 4.4% of the time. Thus, running more ADMM iterations will not considerably increase the training time. If allowed more iterations, the ADMM algorithm will converge to the global optimum of (2.2). In contrast, back-propagation does not have this guarantee due to the non-convexity of (2.1). Moreover, back-propagation is very sensitive to the initializations and hyperparameters. While ADMM also requires a pre-specified step size γ_a , it is much more stable: its convergence to a primal optimum does not depend on the step size [13, Appendix A]. An optimal step size speeds up the training, but a suboptimal step size is also acceptable.

We also compare ADMM with back-propagation on the harder and more modern Fashion MNIST dataset [55]. We perform binary classification between the “pullover” and the “bag”

| Method | Test Accuracy | CPU Time (s) | Training Loss | Global Convergence |
|-----------|---------------|--------------|---------------|--------------------|
| Back-prop | 98.91 % | 62.06 | 437.6 | No |
| CVX | 98.21 % | 14217 | 1.007 | Yes |
| ADMM-RBCD | 98.89 % | 555.8 | 310.3 | Yes |

Table 4: Averaged experiment results with the binary cross-entropy loss on the MNIST dataset over five independent runs. We run 34 ADMM iterations for each setting.

classes on both full data ($n = 12000$, $d = 784$) and downsampled data ($n = 12000$, $d = 196$), with P_s chosen to be 18. The results are presented in Table 3. When the full dataset is considered, ADMM achieves a much lower training loss and a higher test accuracy, but back-propagation is faster. When the downsampled data is considered, ADMM also achieves a lower loss and a higher accuracy, and is even faster than back-propagation. The results show that ADMM is particularly suitable for data whose dimension is around 200.

5.2.4. Binary cross-entropy loss (iterative u updates) – MNIST. To verify the efficacy of using the RBCD method to numerically solve (3.3a), we similarly experiment on the MNIST dataset with the binary cross-entropy loss coupled with a tanh output activation. The resulted loss function is $\ell(\hat{y}, y) = -2\hat{y}^\top y + \mathbf{1}^\top \log(e^{2\hat{y}} + 1)$. Since the value of the full augmented Lagrangian gradient in the stopping condition of Algorithm 3.2 is difficult to obtain, we use the amount of objective improvement as a surrogate. Again, we set P_s to be 24.

The experiment results are shown in Table 4. The ADMM-RBCD algorithm achieves a high test accuracy while requiring a training time 94.6% shorter than the time of globally optimizing the cost function (2.2) with CVX. ADMM-RBCD also requires less time to reach a comparable accuracy than the closed-form ADMM method with the squared loss. On the other hand, ADMM-RBCD is still slower than back-propagation local search, trading the training speed for the global convergence guarantee. The extremely slow pace of CVX forbids its application to even medium-scaled problems, while ADMM-RBCD makes convex training much more practical by balancing between efficiency and optimality.

5.3. Convex adversarial training. Due to space restrictions, we focus on binary classification with the hinge loss, and defer the squared loss results to Appendix B.5.

5.3.1. Hinge loss convex adversarial training – 2D illustration. To analyze the decision boundaries obtained from convex adversarial training, we ran Algorithm 2.1 and Algorithm 4.1 on 34 random points in 2-dimensional space for binary classification. The algorithms were run with the parameters $P_s = 360$ and $\epsilon = 0.08$. A bias term was included by concatenating a column of ones to the data matrix X . The decision boundaries shown in Figure 5 confirm that Algorithm 4.1 fits the perturbation boxes as designed, coinciding with the theoretical prediction [43, Figure 3]. In Appendix B.4, we compare the decision boundaries of convex training methods and back-propagation methods, and discuss how the regularization strength β affects the decision boundaries. Additionally, in Appendix B.3, we compare the convex and the non-convex optimization landscapes and demonstrate robust certifications around

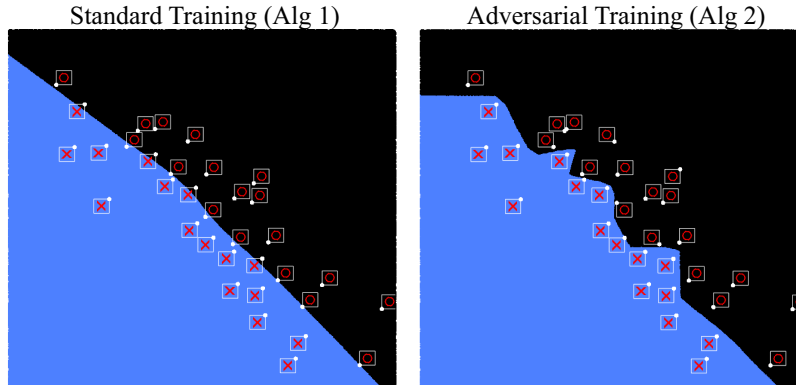


Figure 5: Visualization of the binary decision boundaries in a 2-dimensional space. The red crosses are positive training points while the red circles are negative points. The region classified as positive is in blue, whereas the negative region is in black. The white box around each training data is the ℓ_∞ perturbation bound. The white dot at a vertex of each box is the worst-case perturbation. [Algorithm 4.1](#) fitted the perturbation boxes, while the standard training fitted the training points.

| Method | Clean accuracy | FGSM adv. | PGD adv. | Objective |
|-------------------------------|-----------------|-----------------|------------------|---|
| GD-std | 79.56% (.4138%) | 47.09% (.4290%) | 45.60% (.4796%) | .3146 (.01101) |
| GD-FGSM | 75.30% (3.104%) | 61.03% (4.763%) | 60.99% (4.769%) | .8370 (6.681×10^{-2}) |
| GD-PGD | 76.56% (.6038%) | 62.48% (.2215%) | 62.44% (.1988%) | .8220 (3.933×10^{-3}) |
| Algorithm 2.1 | 81.01% (.8090%) | .4857% (.1842%) | .3571% (.1239%) | 6.910×10^{-3} (3.020×10^{-4}) |
| Algorithm 4.1 | 78.36% (.3250%) | 66.95% (.4564%) | 66.81% (0.4862%) | .6511 (6.903×10^{-3}) |

Table 5: Average optimal objective and accuracy on clean and adversarial data over seven runs on the CIFAR-10 database. The numbers in the parentheses are the standard deviations over the seven runs.

the training data points.

5.3.2. Hinge loss convex adversarial training – image classification. We now verify the real-world performance of the proposed convex training methods on a subset of the CIFAR-10 image classification dataset [37] for binary classification between “birds” and “ships”. The subset consists of 600 images downsampled to $d = 147$.⁶ We use clean data and adversarial data generated with FGSM and PGD to compare the performances of [Algorithm 2.1](#), [Algorithm 4.1](#), traditional back-propagation standard training (abbreviated as GD-std), and the widely-used adversarial training method: use FGSM or PGD to solve for the inner maximum of (4.8) and use back-propagation to solve the outer minimization (abbreviated as GD-FGSM and GD-PGD). The implementation details of FGSM and PGD are discussed in [Appendix C.2](#).

⁶The parameters are $\epsilon = 10$, $\beta = 10^{-4}$, and $P_s = 36$, corresponding to ANN widths of at most 72.

The results on the CIFAR-10 subset are provided in Table 5. Convex standard training (Algorithm 2.1) achieves a higher clean accuracy than GD-std and returns a much lower training loss, supporting the findings of Theorem 2.2. Convex adversarial training (Algorithm 4.1) achieves higher accuracies on clean data and adversarial data compared with GD-FGSM and GD-PGD. While Algorithm 4.1 solves the upper-bound problem (4.10), it returns a lower training objective compared with GD-FGSM and GD-PGD, showing that the back-propagation methods fails to find an optimal network. Moreover, we have observed that Algorithm 2.1 and Algorithm 4.1 are much more stable and are guaranteed to converge to their global optima, while GD-PGD sometimes encounter an oscillatory behavior.

We also compare the aforementioned SDP relaxation adversarial training method [46] and the LP relaxation method [54] against our work on the CIFAR-10 subset. While an iteration of the LP or the SDP method is faster than a GD-PGD iteration, the ANNs trained with the LP or SDP method achieve worse accuracies and robustness than those trained with Algorithm 4.1: the LP method achieves a 74.05% clean accuracy and a 58.65% PGD accuracy, whereas the SDP method achieves 73.35% on clean data and 40.45% on PGD adversaries.⁷ These results support that Algorithm 4.1 trains more robust ANNs and that the LP and SDP relaxations can be extremely loose and unstable. While [46, 54] apply the convex relaxation method to the adversarial training problem, their training formulations are non-convex.

The presence of an ℓ_1 norm term in the upper-bound formulations (4.10) and (4.13) indicates that adversarial training with a small ϵ has a regularizing effect, which can improve generalization, supporting the finding of [38]. In the above experiments, Algorithm 4.1 outperforms Algorithm 2.1 on adversarial data, highlighting the contribution of Algorithm 4.1: a novel convex adversarial training procedure that reliably trains robust ANNs.

6. Concluding Remarks. We use the sampled convex program theory to characterize the quality of the solution obtained from an approximation method, providing theoretical insights into practical convex training. We then develop a separating scheme and applied the ADMM algorithm to the convex training formulation. When combined with the approximation method, the algorithm achieves a quadratic per-iteration computational complexity and a linear convergence towards an approximate global optimum. We also introduced a simpler unconstrained convex training formulation based on an SCP relaxation. The characterization of its solution quality show that ELMs are convex relaxations to ANNs. Compared to the traditional back-propagation algorithms, our proposed training algorithms possess theoretical convergence rate guarantees and enjoy the absence of spurious local minima. Compared with naively solving the convex training formulation using general-purpose solvers, our algorithms have much improved complexities, making a significant step towards practical convex training.

We also use the robust convex optimization analysis to derive convex programs that train adversarially robust ANNs. Compared with traditional adversarial training methods, including GD-FGSM and GD-PGD, the favorable properties of convex optimization endow convex adversarial training with the following advantages:

⁷For SDP, the robustness parameter is chosen as $\lambda = .04$, and larger λ causes the algorithm to fail.

- **Global convergence to an upper bound:** Convex adversarial training provably converges to an upper-bound to the global optimum cost, offering superior interpretability.
- **Guaranteed adversarial robustness on training data:** As shown in [Theorem 4.3](#), the inner maximization over the robust loss function is solved exactly.
- **Hyperparameter-free:** [Algorithm 4.1](#) can automatically determine its step size with line search, not requiring any preset parameters.
- **Immune to vanishing / exploding gradients:** The convex training method avoids this problem completely because it does not rely on back-propagation.

Overall, the analysis of this work makes it easier and more efficient to train interpretable and robust ANNs with global convergence guarantees, potentially facilitating the application of ANNs in safety-critical applications.

References.

- [1] A. AGRAWAL, R. VERSCHUEREN, S. DIAMOND, AND S. BOYD, *A rewriting system for convex optimization problems*, Journal of Control and Decision, 5 (2018), pp. 42–60.
- [2] B. ANDERSON, Z. MA, J. LI, AND S. SOJOUDI, *Tightened convex relaxations for neural network robustness certification*, in IEEE Conference on Decision and Control, 2020.
- [3] B. ANDERSON AND S. SOJOUDI, *Certified robustness via locally biased randomized smoothing*, 2021.
- [4] B. ANDERSON AND S. SOJOUDI, *Data-driven certification of neural networks with random input noise*, 2021.
- [5] M. APS, *The MOSEK optimization toolbox for MATLAB manual. Version 9.0*, 2019.
- [6] R. ARORA, A. BASU, P. MIANY, AND A. MUKHERJEE, *Understanding deep neural networks with rectified linear units*, in International Conference on Learning Representations, 2018.
- [7] A. ATHALYE, N. CARLINI, AND D. WAGNER, *Obfuscated gradients give a false sense of security: Circumventing defenses to adversarial examples*, in International Conference on Machine Learning, 2018.
- [8] F. BACH, *Breaking the curse of dimensionality with convex neural networks*, Journal of Machine Learning Research, 18 (2017), pp. 1–53.
- [9] Y. BAI, T. GAUTAM, Y. GAI, AND S. SOJOUDI, *Practical convex formulation of robust one-hidden-layer neural network training*, 2021.
- [10] A. BECK AND M. TEBoulLE, *A fast iterative shrinkage-thresholding algorithm for linear inverse problems*, SIAM Journal on Imaging Sciences, 2 (2009), pp. 183–202.
- [11] E. BELILOVSKY, M. EICKENBERG, AND E. OYALLON, *Greedy layerwise learning can scale to ImageNet*, in International Conference on Machine Learning, 2019.
- [12] Y. BENGIO, N. ROUX, P. VINCENT, O. DELALLEAU, AND P. MARCOTTE, *Convex neural networks*, in Annual Conference on Neural Information Processing Systems, 2006.
- [13] S. BOYD, N. PARIKH, E. CHU, B. PELEATO, AND J. ECKSTEIN, *Distributed optimization and statistical learning via the alternating direction method of multipliers*, Foundations and Trends in Machine Learning, 3 (2011), pp. 1–122.
- [14] S. BOYD AND L. VANDENBERGHE, *Convex optimization*, Cambridge university press,

- 2004.
- [15] A. BRUTZKUS AND A. GLOBERSON, *Globally optimal gradient descent for a convnet with gaussian inputs*, in International Conference on Machine Learning, 2017.
 - [16] G. CALAFIORE AND M. C. CAMPI, *Uncertain convex programs: randomized solutions and confidence levels*, Mathematical Programming, 102 (2005), pp. 25–46.
 - [17] M. C. CAMPI, S. GARATTI, AND M. PRANDINI, *The scenario approach for systems and control design*, Annual Reviews in Control, 33 (2009), pp. 149–157.
 - [18] J. COHEN, E. ROSENFELD, AND Z. KOLTER, *Certified adversarial robustness via randomized smoothing*, in International Conference on Machine Learning, 2019.
 - [19] S. DIAMOND AND S. BOYD, *CVXPY: A Python-embedded modeling language for convex optimization*, Journal of Machine Learning Research, 17 (2016), pp. 1–5.
 - [20] S. S. DU, X. ZHAI, B. POCZOS, AND A. SINGH, *Gradient descent provably optimizes over-parameterized neural networks*, in International Conference on Learning Representations, 2019.
 - [21] D. DUA AND C. GRAFF, *UCI machine learning repository*, 2017.
 - [22] J. ECKSTEIN AND W. YAO, *Approximate ADMM algorithms derived from lagrangian splitting*, Computational Optimization and Applications, 68 (2017), pp. 363–405.
 - [23] T. ERGEN AND M. PILANCI, *Global optimality beyond two layers: Training deep relu networks via convex programs*, in International Conference on Machine Learning, 2021.
 - [24] T. ERGEN AND M. PILANCI, *Implicit convex regularizers of CNN architectures: Convex optimization of two- and three-layer networks in polynomial time*, in International Conference on Learning Representations, 2021.
 - [25] C. GALLICCHIO AND S. SCARDAPANE, *Deep randomized neural networks*, 2020.
 - [26] I. J. GOODFELLOW, J. SHLENS, AND C. SZEGEDY, *Explaining and harnessing adversarial examples*, in International Conference on Learning Representations, 2015.
 - [27] M. GRANT AND S. BOYD, *CVX: Matlab software for disciplined convex programming, version 2.1*, 2014.
 - [28] K. HE, X. ZHANG, S. REN, AND J. SUN, *Delving deep into rectifiers: Surpassing human-level performance on imagenet classification*, in IEEE International Conference on Computer Vision, 2015.
 - [29] M. R. HESTENES, *Multiplier and gradient methods*, Journal of Optimization Theory and Applications, 4 (1969), pp. 303–320.
 - [30] M. HONG AND Z. LUO, *On the linear convergence of the alternating direction method of multipliers*, Mathematical Programming, 162 (2017), pp. 165–199.
 - [31] K. HORNIK, *Approximation capabilities of multilayer feedforward networks*, Neural Networks, 4 (1991), pp. 251–257.
 - [32] G.-B. HUANG, Q.-Y. ZHU, AND C.-K. SIEW, *Extreme learning machine: a new learning scheme of feedforward neural networks*, in IEEE International Joint Conference on Neural Networks, vol. 2, 2004, pp. 985–990.
 - [33] R. HUANG, B. XU, D. SCHUURMANS, AND C. SZEPESVÁRI, *Learning with a strong adversary*, 2015.
 - [34] S. H. HUANG, N. PAPERNOT, I. J. GOODFELLOW, Y. DUAN, AND P. ABBEEL, *Adversarial attacks on neural network policies*, in International Conference on Learning Representations, 2017.

- [35] B. IGELNIK AND Y. PAO, *Stochastic choice of basis functions in adaptive function approximation and the functional-link net*, IEEE Transactions on Neural Networks, 6 (1995), pp. 1320–1329.
- [36] D. P. KINGMA AND J. BA, *Adam: A method for stochastic optimization*, in International Conference on Learning Representations, 2015.
- [37] A. KRIZHEVSKY, *Learning multiple layers of features from tiny images*, 2012.
- [38] A. KURAKIN, I. J. GOODFELLOW, AND S. BENGIO, *Adversarial machine learning at scale*, in International Conference on Learning Representations, 2017.
- [39] J. LACOTTE AND M. PILANCI, *All local minima are global for two-layer relu neural networks: The hidden convex optimization landscape*, 2020.
- [40] Y. LECUN, C. CORTES, AND C. BURGESS, *Mnist handwritten digit database*, ATT Labs, 2 (2010).
- [41] Z. LU AND L. XIAO, *On the complexity analysis of randomized block-coordinate descent methods*, Mathematical Programming, 152 (2015), pp. 615–642.
- [42] Z. MA AND S. SOJOUDI, *Strengthened SDP verification of neural network robustness via non-convex cuts*, 2020.
- [43] A. MADRY, A. MAKELOV, L. SCHMIDT, D. TSIPRAS, AND A. VLADU, *Towards deep learning models resistant to adversarial attacks*, in International Conference on Learning Representations, 2018.
- [44] S. MOOSAVI-DEZFOOLI, A. FAWZI, AND P. FROSSARD, *Deepfool: A simple and accurate method to fool deep neural networks*, in IEEE Conference on Computer Vision and Pattern Recognition, 2016.
- [45] M. PILANCI AND T. ERGEN, *Neural networks are convex regularizers: Exact polynomial-time convex optimization formulations for two-layer networks*, in International Conference on Machine Learning, 2020.
- [46] A. RAGHUNATHAN, J. STEINHARDT, AND P. LIANG, *Certified defenses against adversarial examples*, in International Conference on Learning Representations, 2018.
- [47] D. E. RUMELHART, G. E. HINTON, AND R. J. WILLIAMS, *Learning representations by back-propagating errors*, Nature, 323 (1986), pp. 533–536.
- [48] A. SAHINER, T. ERGEN, J. M. PAULY, AND M. PILANCI, *Vector-output ReLU neural network problems are copositive programs: Convex analysis of two layer networks and polynomial-time algorithms*, in International Conference on Learning Representations, 2021.
- [49] M. SION, *On general minimax theorems*, Pacific Journal of Mathematics, 8 (1958), p. 171–176.
- [50] C. SZEGEDY, W. ZAREMBA, I. SUTSKEVER, J. BRUNA, D. ERHAN, I. J. GOODFELLOW, AND R. FERGUS, *Intriguing properties of neural networks*, in International Conference on Learning Representations, 2014.
- [51] G. TAYLOR, R. BURMEISTER, Z. XU, B. SINGH, A. PATEL, AND T. GOLDSTEIN, *Training neural networks without gradients: A scalable admm approach*, in 33rd International Conference on Machine Learning, 2016.
- [52] L. VENTURI, A. S. BANDEIRA, AND J. BRUNA, *Spurious valleys in one-hidden-layer neural network optimization landscapes*, Journal of Machine Learning Research, 20 (2019), pp. 1–34.

-
- [53] J. WANG, F. YU, X. CHEN, AND L. ZHAO, *ADMM for efficient deep learning with global convergence*, in ACM SIGKDD International Conference on Knowledge Discovery & Data Mining, 2019.
 - [54] E. WONG AND Z. KOLTER, *Provable defenses against adversarial examples via the convex outer adversarial polytope*, in International Conference on Machine Learning, 2018.
 - [55] H. XIAO, K. RASUL, AND R. VOLLGRAF, *Fashion-mnist: a novel image dataset for benchmarking machine learning algorithms*, 2017.

Appendix A. SCP-based Convex Training.

While the practical training formulation (2.5) and the ADMM algorithm (Algorithm 3.1) vastly improve the efficiency and the practicality of globally optimizing ANNs, the complexity of the aforementioned methods can still be too high for large-scale machine learning problems due to the complicated structure of (2.2). In this section, we propose a “sampled convex program (SCP)”-based alternative approach to approximately globally optimize scalar-output one-hidden-layer ANNs. This approach constructs scalable unconstrained convex optimization problems with simpler structures. Unconstrained convex optimization problems are much easier to numerically solve compared to constrained ones. Scalable and simple first-order methods can be easily applied to unconstrained convex programs, while the same cannot be said for constrained optimization in general due to feasibility issues.

Compared with the ADMM approach in Algorithm 3.1, the SCP approach is easier to implement and has a lower per-iteration complexity. The trade-off is that while Algorithm 3.1 can be applied to find the exact global minimum of (2.1) (albeit with an exponential complexity with respect to the data matrix rank), the SCP approach only finds an approximately global solution. In the approximate case, the qualities of the ADMM solution and the SCP solution can both be characterized.

A.1. One-shot sampling of hidden-layer weights. The paper [45] has shown that the non-convex training formulation (2.1) has the same global optimum as

$$(A.1) \quad p^* = \min_{(u_j, \alpha_j)_{j=1}^m} \ell \left(\sum_{j=1}^m (X u_j)_+ \alpha_j, y \right) + \frac{\beta}{2} \sum_{j=1}^m |\alpha_j| \quad \text{s. t.} \quad \|u_j\|_2 \leq 1, \forall j \in [m].$$

Note that we can replace the perturbation set $\{u \mid \|u\|_2 \leq 1\}$ with $\{u \mid \|u\|_2 = 1\}$ without changing the optimum. This is because for any pair (u_j, α_j) such that $\|u_j\|_2 < 1$, replacing (u_j, α_j) with the scaled weights $(\frac{u_j}{\|u_j\|_2}, \|u_j\|_2 \cdot \alpha_j)$ will reduce the regularization term of (A.1) while keeping the loss term unchanged. Therefore, the optimal u_j^* must satisfy $\|u_j^*\|_2 = 1$.

To approximate the semi-infinite program (A.1), we randomly sample a total of N vectors, namely u_1, \dots, u_N , on the ℓ_2 unit norm sphere \mathcal{S}^{d-1} following a uniform distribution. It is well-known that such a procedure can be performed by randomly sampling $\hat{u}_i \sim \mathcal{N}(0, I_d)$ for all $i \in [N]$ and projecting each \hat{u}_i onto the unit ℓ_2 norm sphere by calculating $u_i = \frac{\hat{u}_i}{\|\hat{u}_i\|_2}$ for all $i \in [N]$. Next, u_1, \dots, u_N are used to construct the following SCP:

$$(A.2) \quad p_{s3}^* = \min_{(\alpha_i)_{i=1}^N} \ell \left(\sum_{i=1}^N (X u_i)_+ \alpha_i, y \right) + \beta \sum_{i=1}^N |\alpha_i|,$$

where the sampled hidden-layer weights $(u_i)_{i=1}^N$ are fixed.

The finite-dimensional unconstrained convex formulation (A.2) is a relaxation of (A.1), and can be used as a surrogate for the optimization (2.1) to approximately globally optimize one-hidden-layer ANNs. The formulation (A.2) optimizes the output layer of the ANN while keeping the hidden layer fixed. When the squared loss $\ell(\hat{y}, y) = \frac{1}{2} \|\hat{y} - y\|_2^2$ is considered, (A.2)

is a Lasso regression problem. Intuitively, the sampled hidden-layer weights transform the training data points into a higher-dimensional space. While some of the sampled weights will inevitably be far from the optimum weights for the ANN, the ℓ_1 regularization term promotes sparsity, encouraging assigning zero weights to “disable” the suboptimal hidden neurons.

The SCP training formulation (A.2) recovers the training problems of one-hidden-layer random vector functional link (RVFL) [35] and ELM. Such an equivalence shows that training an ELM is a convex relaxation to training an ANN. Compared with traditional ELMs, (A.2) contains a sparsity-promoting regularization, and requires a different initialization of the untrained hidden layer weights, providing insights into the implicit sparsity-seeking property of ANNs.

The method in this subsection is referred to as “one-shot sampling” because all hidden layer weights are sampled in advance, in contrast with the iterative sampling procedure described in Appendix A.2. The ANNs trained with (A.2) can be suboptimal in terms of empirical loss compared with the network that globally minimizes the non-convex cost function, but are expected to be close to the optimal classifier. The next theorem characterizes the level of suboptimality of the SCP optimizer, with the proof provided in Appendix E.3.

Theorem A.1. *Suppose that an additional hidden neuron u_{N+1} is randomly sampled on the unit Euclidean norm sphere via a uniform distribution to augment the ANN. Consider the following formulation to train the augmented network:*

$$(A.3) \quad p_{s4}^* = \min_{(\alpha_i)_{i=1}^{N+1}} \ell \left(\sum_{i=1}^{N+1} (Xu_i)_+ \alpha_i, y \right) + \beta \sum_{i=1}^{N+1} |\alpha_i|.$$

It holds that $p_{s4}^ \leq p_{s3}^*$. Furthermore, if $N \geq \min \left\{ \frac{n+1}{\psi\xi} - 1, \frac{2}{\xi}(n+1 - \log \psi) \right\}$, where ψ and ξ are preset confidence level constants between 0 and 1, then with probability no smaller than $1 - \xi$, it holds that $\mathbb{P}\{p_{s4}^* < p_{s3}^*\} \leq \psi$.*

Intuitively, this bound means that uniformly sampling another hidden layer weight u_{N+1} on the unit norm sphere will not improve the training loss with high probability. For a fixed level of suboptimality, the required scale of the SCP formulation (A.2) has a linear relationship with respect to the number of training data points. Somewhat surprisingly, from the perspective of the probabilistic optimality, the bound provided by Theorem A.1 is the same as the bound associated with Algorithm 2.1 presented in Theorem 2.2, because both bounds are obtained via the SCP analysis framework.

The main advantage of the SCP-based training approach is that the unconstrained optimization (A.2) is much easier and faster to solve than the constrained optimization (2.5). The iterative soft-thresholding algorithm (ISTA) [10] and its accelerated or stochastic variants can be readily applied to solve (A.2). Specifically, ISTA converges at a linear rate if $\ell(\sum_{i=1}^N (Xu_i)_+ \alpha_i, y)$ is strongly convex over each α_i , and converges at a $\mathcal{O}(1/T)$ rate for weakly convex cases, where T is the iteration count. As a result, with the same amount of computational resources, one can solve (A.2) with $N \gg P_s$, allowing for training wider networks (with stronger representation powers) within a reasonable amount of time. Numerical experiments in Appendix B.2 verify that the SCP relaxation (A.2) can train larger-scale classifiers with a reasonable computing effort.

When $\ell(\cdot)$ is the squared loss, the SCP formulation (A.2) evaluates to $\min_{\alpha} \|H\alpha - y\|_2^2 + \beta \|\alpha\|_1$, where $H = [(Xu_1)_+ \ \dots \ (Xu_N)_+] \in \mathbb{R}^{n \times N}$ and $\alpha = (\alpha_1, \dots, \alpha_N) \in \mathbb{R}^N$. The ISTA update is then $\alpha^+ = \text{prox}_{\gamma_s \beta \|\cdot\|_1}(\alpha - \gamma_s H^\top H \alpha + \gamma_s H^\top y)$, where $\text{prox}_{\gamma_s \beta \|\cdot\|_1}(\cdot)$ evaluates to $\text{sgn}(\cdot) \max(|\cdot| - \gamma_s \beta, 0)$, α^+ denotes the updated α at each iteration, and γ_s is a step size that can be determined with backtracking line search. Since $H^\top H$ and $H^\top y$ are fixed and only need to be calculated once, the per-iteration complexity is $\mathcal{O}(N^2)$. Since N is linear in n for a fixed solution quality (cf. Theorem A.1), the per-iteration complexity amounts to $\mathcal{O}(n^2)$, and the overall complexity amounts to $\mathcal{O}(n^2 \log(1/\epsilon_a))$ and $\mathcal{O}(n^2/\epsilon_a)$ for strongly and weakly convex loss functions, respectively, where ϵ_a is the desired optimization precision.

Theorem 2.2 also implies that when the neural network is wide, the hidden layer weights are less important than the output layer weights. The role of the hidden layers is to map the data to features in higher-dimensional spaces, facilitating the output layer to extract the most important information.

A.2. Iterative sampling of hidden-layer weights. While the efficacy of the SCP-based convex training formulation with a one-shot sampling of the hidden layer neurons can be proved theoretically and experimentally, the probabilistic optimality bound provided in Theorem A.1 may be too conservative in some cases. To provide a more accurate and robust estimation of the level of suboptimality of the SCP relaxation (A.2), we propose a scheme (Algorithm A.1) that iteratively samples hidden layer neurons used in (A.2) to train classifiers.

The convex semi-infinite training formulation (A.1) has a dual problem: [45, Appendix A.4]

$$(A.4) \quad d^* = \max_{v \in \mathbb{R}^n} -\ell^*(v) \quad \text{s. t.} \quad |v^\top (Xu)_+| \leq \beta, \quad \forall u : \|u\|_2 \leq 1,$$

where $\ell^*(\cdot)$ is the Fenchel conjugate function defined as $\ell^*(v) = \max_z z^\top v - \ell(z, y)$. When $m \geq m^*$, where m^* is upper-bounded by $n + 1$, strong duality holds $p^* = d^*$. Moreover, the dual problem (A.4) is a convex semi-infinite problem, which is a category of uncertain convex programs (UCP) [16].

We then use the sampled vectors u_1, \dots, u_N to construct the following SCP that approximates the UCP (A.4):

$$(A.5) \quad d_{s3}^* = \max_{v \in \mathbb{R}^n} -\ell^*(v) \quad \text{s. t.} \quad |v^\top (Xu_i)_+| \leq \beta, \quad \forall i \in [N].$$

Similarly, strong duality holds between (A.5) and (A.2) and it holds that $p_{s3}^* = d_{s3}^*$. The level of suboptimality of the dual solution v^* to (A.5) can be easily verified by checking the feasibility of v^* to the UCP (A.4).

While it is easier to check the quality of the dual solution, it is desirable to solve the primal problem (A.2) because the primal is unconstrained and thus easier to solve. Suppose that $(\alpha_i^*)_{i=1}^N$ is a solution to (A.2). By following the procedure described in Appendix E.4, one can recover the optimal dual variable v^* from $(\alpha_i^*)_{i=1}^N$ by exploiting the strong duality between (A.2) and (A.5). Next, we independently sample another set of N_1 hidden layer weights

$(u_i^1)_{i=1}^{N_1} \sim \text{Unif}(\mathcal{S}^{n-1})$ and check if $|v^{\star\top}(Xu_i^1)_+| > \beta$ for each $i \in [N_1]$. If $|v^{\star\top}(Xu_i^1)_+| > \beta$ for a particular i , then adding u_i^1 to the set of sampled constraint set of (A.5) will change (reduce) the value of $d_{s_3}^*$ and thereby reduce the relaxation gap between $p_{s_3}^*$ and p^* . In other words, by incorporating u_i^1 as another hidden layer node, the considered ANN can be improved.

Define the notations

$$Z_i := \begin{cases} 1 & \text{if } |v^{\star\top}(Xu_i^1)_+| > \beta \\ 0 & \text{otherwise} \end{cases}, \text{ for all } \forall i \in [N_1],$$

$$\bar{Z} := \frac{\sum_{i=1}^{N_1} Z_i}{N_1}, \quad \text{and} \quad \theta := \mathbb{E}_{u \sim \text{Unif}(\mathcal{S}^{d-1})}[Z_i] = \mathbb{P}_{u \sim \text{Unif}(\mathcal{S}^{d-1})}[|v^{\star\top}(Xu)_+| > \beta].$$

By Hoeffding's inequality, it holds that $\mathbb{P}(\theta - \bar{Z} \geq t) \leq \exp(-2N_1 t^2)$. Therefore, with probability at least $1 - \xi$, it holds that $\theta \leq \bar{Z} + \frac{\log(1/\xi)}{2N_1}$, where $\xi \in (0, 1]$. In other words, by evaluating the feasibility of the additional set of hidden layer weights $u_1^1 \dots u_{N_1}^1$, one can obtain a probabilistic bound on the level of suboptimality of the solution to (A.5) constructed with $u_1 \dots u_N$: as long as $\bar{Z} + \frac{\log(1/\xi)}{2N_1} \leq \psi$ for a constant $\psi \in (0, 1]$, it holds that $\theta \leq \psi$ with probability at least $1 - \xi$.

We now introduce a scheme of training scalar-output fully-connected ReLU ANNs to an arbitrary degree of suboptimality by repeating the evaluation and sampling procedure, described in Algorithm A.1. Let T denote the total iterations of Algorithm A.1, U_t denote the total number of hidden layer neurons at iteration t , and N_t denote the number of hidden layer neurons sampled at iteration t . In light of Theorem A.1, it holds that the solution $(\alpha_i^*)_{i=1}^{U_T}$ yielded by Algorithm A.1 satisfies the following property with probability at least $1 - \xi$: if an additional vector \tilde{u} is sampled on the unit Euclidean norm sphere \mathcal{S}^{d-1} via a uniform distribution, then adding \tilde{u} to the set of hidden layer weights used in (A.2) will not improve the training loss of the ANN with probability at least $1 - \psi$.

Appendix B. Additional Experiments.

B.1. ADMM asymptotic convergence. In this part of the appendix, we present empirical evidences that demonstrate the asymptotic convergence properties of ADMM (Algorithm 3.1). We use the same data as in subsection 5.2.1, and the experiment settings are presented in Appendix C.1.

Figure 6a shows that the training loss converges to a stationary value at a linear rate, verifying the findings of Theorem 3.1. Note that the D_h matrices randomly generated in the five runs are different, resulting in different optimization landscapes and different linear convergence bounds. Figure 6b shows that ADMM converges towards the CVX ground truth, verifying the correctness of the ADMM solution. Figure 6c shows that $l_{\text{ADMM}}^{\nu,w}$ and $l_{\text{ADMM}}^{u,\alpha}$ are close throughout the ADMM iterations, implying that v_i and w_i violate the constraints of (2.2) insignificantly at every step. Together, these figures confirm that the ADMM algorithm optimizes (2.1) effectively as designed. The learning curves of the five runs look quite different because different random D_h matrices can make the optimization landscape quite different. However, as illustrated in Figure 2, the initial rapid convergence behavior is very consistent.

Algorithm A.1 Convex ANN training based on iterative sampling hidden-layer weights

- 1: Let $t = 0$; sample $\hat{u}_1^0, \dots, \hat{u}_{N_0}^0 \sim \mathcal{N}(0, I_d)$ i.i.d., and let $u_i^0 = \frac{\hat{u}_i^0}{\|\hat{u}_i^0\|_2}$ for all $i \in [N_0]$.
- 2: Construct $\mathcal{U}^0 := \{u_1^0, \dots, u_{N_0}^0\}$; let $U_0 = N_0$.
- 3: **repeat**
- 4: Solve $(\alpha_i^t)_{i=1}^{U_t} = \arg \min_{(\alpha_i)_{i=1}^{U_t}} \ell(\sum_{i=1}^{U_t} (Xu_i^t)_+ \alpha_i, y) + \beta \sum_{i=1}^{U_t} |\alpha_i|$, the same formulation as (A.2).
- 5: Update $v^t = y - \sum_{i=1}^{U_t} (Xu_i^t)_+ \alpha_i^t$.
- 6: Sample $\hat{u}_1^{t+1}, \dots, \hat{u}_{N_{t+1}}^{t+1} \sim \mathcal{N}(0, I_d)$ i.i.d., and let $\bar{u}_i^{t+1} = \frac{\hat{u}_i^{t+1}}{\|\hat{u}_i^{t+1}\|_2}$ for all $i \in [N_{t+1}]$.
- 7: Construct $\mathcal{E}^{t+1} = \{\bar{u}_i^{t+1} \mid |v^{t\top} (X\bar{u}_i^{t+1})_+| > \beta\}$ to be the set of newly sampled weight vectors that tighten the dual constraint.
- 8: Construct $\mathcal{U}^{t+1} = \mathcal{U}^t \cup \mathcal{E}^{t+1}$ and rename all vectors in \mathcal{U}^{t+1} as $u_1^{t+1}, \dots, u_{U_{t+1}}^{t+1}$, where U_{t+1} is the cardinality of \mathcal{U}^{t+1} .
- 9: $t \leftarrow t + 1$.
- 10: **until** $\frac{|\mathcal{E}^t|}{N_t} + \frac{\log(1/\xi)}{2N_t} \leq \psi$ or/and $U_{t-1} \geq \frac{n+1}{\psi\xi} - 1$, where ψ and ξ are preset thresholds.

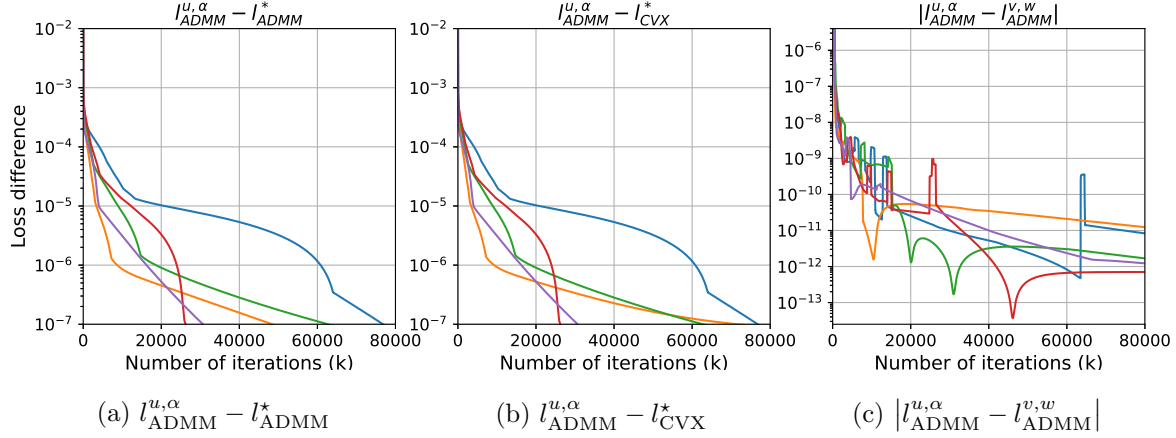


Figure 6: Gap between the cost returned by ADMM at each iteration and the true optimal cost for five independent runs.

B.2. The SCP convex training formulation. In this subsection, we demonstrate the efficacy of the SCP relaxed training using the one-shot random sampling approach to choose u_1, \dots, u_N and explore the effect of the number of sampled weights N . We independently sample different numbers of hidden-layer-weights and use the SCP training formulation (A.2) to train ANNs on the “mammographic masses” dataset [21]. We remove instances containing NaNs and randomly select 70% of the data for the training set and 30% for the test set, resulting in $n = 581$ and $d = 5$. We use two different regularization strengths: $\beta = 10^{-4}$ and $\beta = 10^{-2}$. The training loss and the test accuracy of each N setting are plotted in Figure 7. The ANN training process is stochastic due to the randomly generated hidden-layer weights

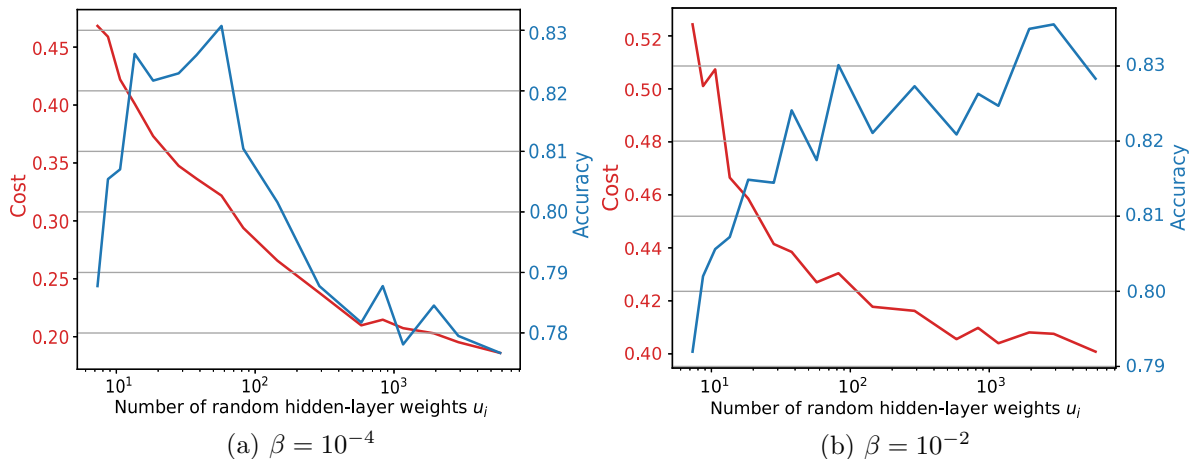
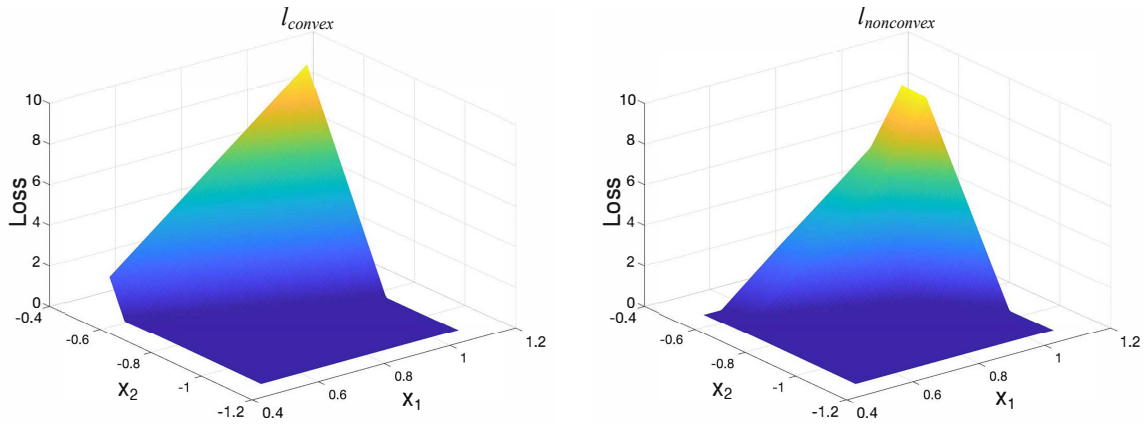


Figure 7: Average accuracy and average cost with different choices of N for two different selections of the regularization strength β .

u_j and the random splitting of training and test sets. We use CVXPY and the MOSEK solver to solve the underlying optimization problem (A.2). We perform 20 independent trials for each N and average the results.

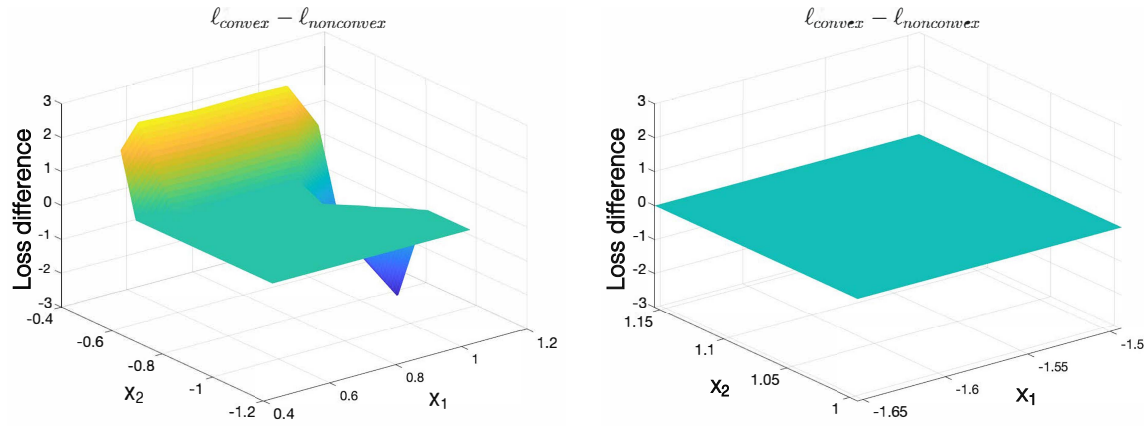
For both regularization settings, adding more sampled hidden layer weights makes the SCP approximation more refined and therefore decreases the training loss. When the regularization strength β is 10^{-4} , the test accuracy increases, peaks, and then decreases as N increases. The accuracy drops when N is large possibly because of the overfitting caused by a lack of sparsity. As a comparison, training ANNs using Algorithm 2.1 with P_s set to 120 achieves an average accuracy of 79.80% and an average training loss of 0.2428 on the same dataset. Directly optimizing the non-convex cost function (2.1) using gradient descent back-propagation with the width m set to $2P_s = 240$ achieves a 81.14% average test accuracy and a 0.3560 average cost. Thus, with a proper choice of N , the prediction performance of the SCP convex training approach is on par with Algorithm 2.1 and traditional back-propagation SGD. When the regularization strength β is 10^{-2} , the test accuracy of the ANNs trained with the SCP method generally increases with N .

To verify the performance of the proposed training approach on larger-scale data, we use the SCP method to train ANNs on the MNIST handwritten digits database [40] for binary classification between digits “2” and “8” ($d = 784$ and $n = 11809$) using the binary cross-entropy loss. The SCP training formulation (A.2) is solved with the ISTA algorithm [10]. With the number of sampled weights N set to 39365 (a much larger value than P_s in the ADMM experiments, corresponding to an optimality level of $\xi\psi = 0.3$), the SCP formulation (A.2) achieves a test accuracy of 99.45%. Compared with the ADMM approach discussed in section 3, the SCP formulation is able to train much wider ANNs with a similar amount of computational power. In summary, this result demonstrates the performance and efficiency advantage of the SCP formulation (A.2) for medium or large machine learning problems.



(a) The loss landscape of the convex objective ℓ_{convex} for $\|\delta\|_\infty \leq 0.3$.

(b) The loss landscape of the non-convex objective $\ell_{\text{nonconvex}}$ for $\|\delta\|_\infty \leq 0.3$.



(c) $\ell_{\text{convex}} - \ell_{\text{nonconvex}}$ for $\|\delta\|_\infty \leq 0.3$.

(d) $\ell_{\text{convex}} - \ell_{\text{nonconvex}}$ zoomed into $\|\delta\|_\infty \leq 0.08$.

Figure 8: Illustrations of the optimization landscapes of the convex and non-convex training formulations.

B.3. Hinge loss convex adversarial training – the optimization landscape. This subsection shows that the convex loss landscape and the non-convex landscape overlap within an ℓ_∞ -norm-bounded additive perturbation set around a training point x_k , and thereby verifies that the convex objective (5.4a) provides an exact certification of the non-convex loss function at training data points.

The visualizations are based on the 2-dimensional experiment described in subsection 5.3.1. We use Algorithm 4.1 to train a robust ANN on the 2-dimensional dataset with $\epsilon = 0.08$, $P_s = 360$, and $\beta = 10^{-9}$. We then randomly select one of the training points x_k and plot the loss around x_k for the convex objective (5.4a) and the non-convex objective (4.1). Specifically,

for $\|\delta\|_\infty \leq 0.3$, we plot

$$\ell_{\text{convex}} = \left(1 - y_k \cdot \sum_{i=1}^P d_{ik}(x_k + \delta)^\top (v_i^* - w_i^*)\right) \text{ and } \ell_{\text{nonconvex}} = \left(1 - y_k \cdot \sum_{j=1}^m ((x_k + \delta)^\top u_j^*)_+ \alpha_j^*\right),$$

where d_{ik} is the k^{th} entry of D_i , y_k is the training label corresponding to x_k . Moreover, v_i^* , w_i^* are the optimizers returned by [Algorithm 4.1](#) and u_j^* and α_j^* are the ANN weights recovered from v_i^* and w_i^* with [\(2.4\)](#). The plots are shown in [Figure 8a, 8b](#).

For a clearer visualization, we also plot $\ell_{\text{convex}} - \ell_{\text{nonconvex}}$ in [Figure 8c](#) and zoom in to the ℓ_∞ norm ball with radius $\epsilon = 0.08$ in [Figure 8d](#). When $\ell_{\text{convex}} - \ell_{\text{nonconvex}}$ is zero, the convex objective provides an exact certificate for the non-convex loss function. [Figure 8d](#) shows that for $\|\delta\|_\infty \leq 0.08$, the difference is zero, supporting the finding that for ANNs trained with [Algorithm 4.1](#), the convex objective offers an exact certificate around the training points.

B.4. Hinge loss convex adversarial training with different regularizations. We now compare the decision boundaries obtained from the convex training algorithms and back-propagation algorithms. As shown in [Figure 9](#), the two standard training methods ([Algorithm 2.1](#) and GD-std) learned decision boundaries that separated the training points but failed to separate the perturbation boxes. Note that [Algorithm 2.1](#) learned slightly more sophisticated boundaries while GD-std learned near-linear boundaries that were very close to one of the positive training points \times .

The convex adversarial training method given by [Algorithm 4.1](#) learns boundaries that separate all perturbation boxes when β was 10^{-3} , 10^{-6} , or 10^{-9} . This behavior matches the theoretical illustration of adversarial training [[43](#), [Figure 3](#)], and verifies that [Algorithm 4.1](#) works as intended. When the regularization is too strong ($\beta = 10^{-2}$), the robust boundary becomes smoothed out and very similar to the standard training boundaries. The traditional adversarial training method GD-PGD learns boundaries that separated most perturbation boxes. However, the boundaries cut through the box at around $(1, -1)$ when β is 10^{-3} , 10^{-6} , or 10^{-9} . This behavior is likely caused by GD-PGD’s worse convergence due to the non-convexity. When β is too large, the GD-PGD boundary also becomes smoothed out.

B.5. Squared loss convex adversarial training. The performance of the proposed robust optimization problem [\(D.4\)](#) is compared with the standard training problem [\(2.2\)](#) on an illustrative 1-dimensional dataset. [Figure 10](#) shows the true relationship between the data vector X and the target output y . Training data are constructed by uniformly sampling eight points from this distribution, and test data are constructed by uniformly sampling 100 points. A bias term is included by concatenating a column of ones to X .

The training and test procedure are repeated for 100 trials with convex standard training ([Algorithm 2.1](#)). For convex adversarial training ([Algorithm 4.1](#)), we varied the perturbation radius $\epsilon = 0.1, \dots, 0.9$. The training and test procedure was carried out for ten trials for each ϵ . [Figure 11](#) reports the average test mean square error (MSE) for each setup.

The adversarial training procedure outperforms standard training for all ϵ choices. We further

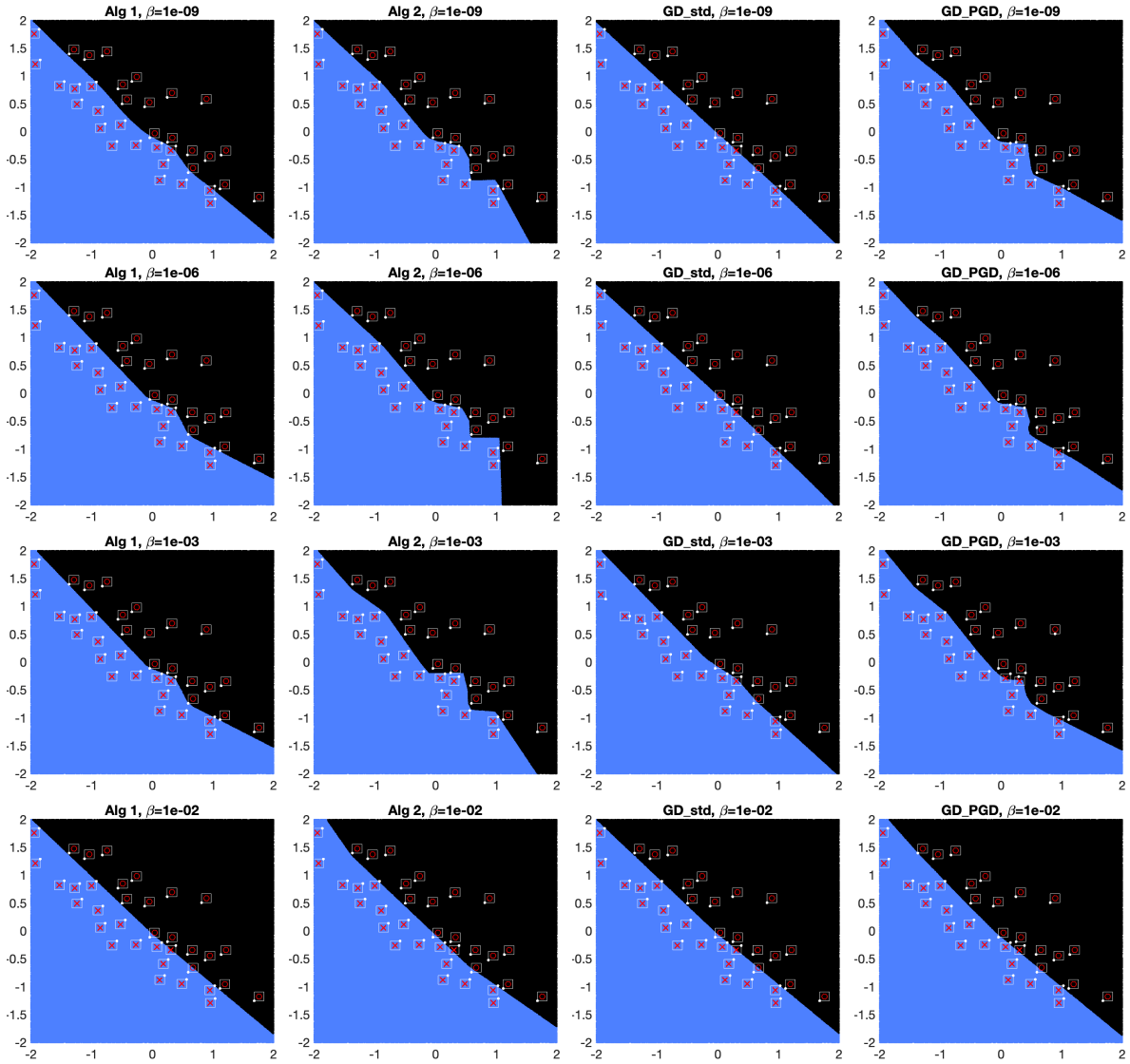


Figure 9: Decision boundaries obtained from various methods with β set to 10^{-9} , 10^{-6} , 10^{-3} , and 10^{-2} .

observe that the average MSE is the lowest at $\epsilon \approx 0.3$. This behavior arises as the robust problem attempts to account for all points within the uncertainty interval around the sampled training points. When ϵ is too small, the robust problem approaches the standard training problem. Larger values of ϵ cause the uncertainty interval to overestimate the constant regions of the true distribution, increasing the MSE.

Appendix C. Experiment Setting Details.

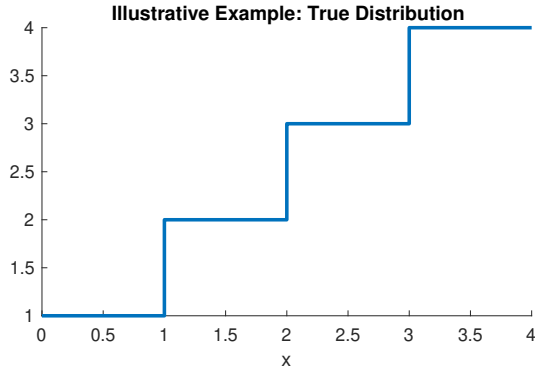


Figure 10: The true relationship between the data x and the targets y used in the illustrative example in Appendix B.5. The training ($n = 8$ points) and test ($n = 100$ points) sets are uniformly sampled from the distribution.

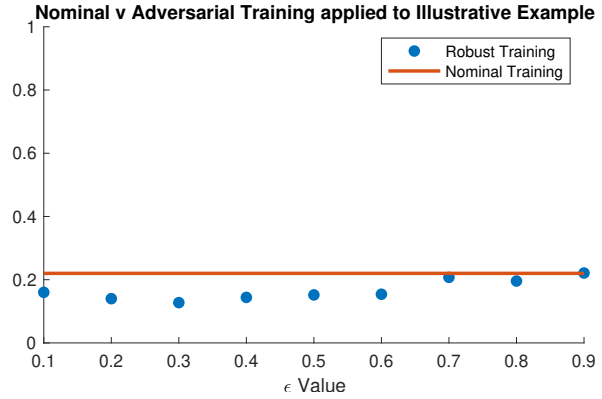


Figure 11: The robust training approach (D.4) outperforms the standard approach for different $\epsilon \in \{0.1, \dots, 0.9\}$ on the dataset studied in Appendix B.5.

| | Figure 6 | Figure 2 | Figure 3 | Figure 4 | Table 2 | Table 4 |
|------------|----------|----------|----------|----------|---------|---------|
| ρ | 0.4 | 0.4 | 0.1 | 0.1 | 0.1 | 0.01 |
| γ_a | 0.01 | 0.4 | 0.1 | 0.1 | 0.1 | 0.01 |
| β | 0.0005 | 0.0005 | 0.0005 | 0.0001 | 0.001 | 0.001 |

Table 6: Hyperparameter settings used for the ADMM experiments.

C.1. ADMM hyperparameters. The proposed ADMM algorithm has two hyperparameters: a penalty hyperparameter ρ and a step size γ_a . The hyperparameters used in the experiments in this paper are shown in Table 6. In most experiments, we selected $\gamma_a = \rho$, a common choice for the ADMM algorithm. The penalty parameter ρ controls the level of infeasibility of v and w . Note that while ADMM guarantees to converge to an optimal feasible solution, the optimization variables may be infeasible in intermediate steps. The feasibility of v_i and w_i to (2.2) is emphasized when ρ is large, while a low objective value is emphasized when ρ is small. For the purpose of finding optimal u_j and α_j that minimize (2.1), a balance between feasibility and low objective is required. In practice, if there exists a significant gap between the objective of (2.2) and the training loss (2.1), then ρ should be increased. If the objective of (2.2) struggles to reduce, then ρ should be decreased.

C.2. FGSM and PGD details. The hinge loss has a flat part that has a zero gradient. To generate adversarial examples even in this part, we treat it as the “leaky hinge loss” via the model $\max\{\zeta(1 - \hat{y} \cdot y), 1 - \hat{y} \cdot y\}$, where $\zeta \rightarrow 0^+$. Hence, the FGSM calculation (4.2) amounts to

$$\tilde{x} = x - \epsilon \cdot \text{sgn}\left(y \cdot \sum_j: x^\top u_j \geq 0 (u_j \alpha_j)\right).$$

Similarly, the PGD update (4.3) evaluates to

$$\tilde{x}^{t+1} = \Pi_{\mathcal{X}} \left(\tilde{x}^t - \gamma_p \cdot \text{sgn} \left(y \cdot \sum_{j: x^\top u_j \geq 0} (u_j \alpha_j) \right) \right), \quad \tilde{x}^0 = x.$$

where the projection step can be performed by clipping the coordinates that deviate more than ϵ from x . In the following experiments, we use $\gamma_p = \epsilon/30$ and run PGD for 40 steps.

Appendix D. Extensions.

D.1. Convex squared loss adversarial training. The squared loss $\ell(\hat{y}, y) = \frac{1}{2} \|\hat{y} - y\|_2^2$ is another commonly used loss function in machine learning. Consider the non-convex training problem of a one-hidden-layer ReLU ANN trained with the ℓ_2 -regularized squared loss:

$$(D.1) \quad \min_{(u_j, \alpha_j)_{j=1}^m} \frac{1}{2} \left\| \sum_{j=1}^m (X u_j)_+ \alpha_j - y \right\|_2^2 + \frac{\beta}{2} \sum_{j=1}^m (\|u_j\|_2^2 + \alpha_j^2).$$

Coupling this nominal problem with the perturbation set \mathcal{X} gives us the robust counterpart as

$$(D.2) \quad \min_{(u_j, \alpha_j)_{j=1}^m} \left(\max_{\Delta: X+\Delta \in \mathcal{X}} \frac{1}{2} \left\| \sum_{j=1}^m ((X + \Delta) u_j)_+ \alpha_j - y \right\|_2^2 + \frac{\beta}{2} \sum_{j=1}^m (\|u_j\|_2^2 + \alpha_j^2) \right).$$

Applying [Theorem 4.1](#) and [Corollary 4.2](#) leads to the following formulation as an upper bound on (D.2):

$$(D.3) \quad \min_{(v_i, w_i)_{i=1}^{\hat{P}}} \left(\max_{\Delta: X+\Delta \in \mathcal{X}} \frac{1}{2} \left\| \sum_{i=1}^{\hat{P}} D_i (X + \Delta) (v_i - w_i) - y \right\|_2^2 + \beta \sum_{i=1}^{\hat{P}} (\|v_i\|_2 + \|w_i\|_2) \right)$$

s. t. $(2D_i - I_n) X v_i \geq \epsilon \|v_i\|_1, \quad (2D_i - I_n) X w_i \geq \epsilon \|w_i\|_1, \quad \forall i \in [\hat{P}].$

Solving the maximization over Δ in closed form leads to the next result, with the proof provided in [Appendix E.8](#).

Theorem D.1. *The optimization problem (D.3) is equivalent to the convex program:*

$$(D.4) \quad \min_{(v_i, w_i)_{i=1}^{\hat{P}}, a, z} a + \beta \sum_{i=1}^{\hat{P}} (\|v_i\|_2 + \|w_i\|_2)$$

s. t. $(2D_i - I_n) X v_i \geq \epsilon \|v_i\|_1, \quad (2D_i - I_n) X w_i \geq \epsilon \|w_i\|_1, \quad \forall i \in [\hat{P}]$

$$z_k \geq \left| \sum_{i=1}^{\hat{P}} D_{ik} x_k^\top (v_i - w_i) - y_k \right| + \epsilon \left\| \sum_{i=1}^{\hat{P}} D_{ik} (v_i - w_i) \right\|_1, \quad \forall k \in [n]$$

$$z_{n+1} \geq \left| 2a - \frac{1}{4} \right|, \quad \|z\|_2 \leq 2a + \frac{1}{4}.$$

Problem (D.4) is a convex optimization that can train robust ANNs. However, directly using (D.4) for adversarial training can be intractable due to the large number of constraints that arise when we include all D_i matrices associated with all Δ such that $X + \Delta \in \mathcal{X}$. To this end, one can use the approximation in Algorithm 4.1 and sample a subset of the diagonal matrices D_1, \dots, D_{P_s} . As before, the optimality gap can be characterized with Theorem 2.2.

D.2. More advanced ANN structures. While our discussions explicitly focus on one-hidden-layer scalar-output ReLU networks, the derived training methods can be used for more sophisticated ANN architectures. As discussed above, greedily training one-hidden-layer ANNs leads to a well-performing deep network [11]. Leveraging recent works that reform the training of more complex ANNs into convex programs [24, 23, 48], our analysis can also extend to those ANNs because most convex training formulations share similar structures. Specifically, these convex training formulations rely on binary matrices to represent ReLU activation patterns and rely on convex (and often linear) constraints to enforce the patterns, with different regularizations revealing the sparse properties of different architectures. Coupling layer-wise training [11] and SCP convex training recovers multi-layer ELMs.

As an example, we now extend our convex adversarial training analysis to various CNN formulations used in [24].

The paper [24] shows that the convex ANN training approach extends to various CNN architectures. Taking advantage of this result, the convex adversarial training formulations similarly generalize. In this part of the appendix, we change our notations to align with [24]. For example, the robust counterpart of the average pooling two-layer CNN convex training formulation (cf. Equations (4) and (26) in [24]) is:

$$\begin{aligned} \min_{\{v_i, w_i\}_{i=1}^{P_{\text{conv}}}} & \left(\max_{X_k \in \mathcal{X}_k} \ell \left(\sum_{i=1}^{P_{\text{conv}}} \sum_{k=1}^K \bar{D}_i^k X_k (w_i - v_i), \mathbf{y} \right) + \beta \sum_{i=1}^{P_{\text{conv}}} (\|v_i\|_2 + \|w_i\|_2) \right) \\ \text{s.t.} & \quad \min_{X_k \in \mathcal{X}_k} (2\bar{D}_i^k - I_n) X_k w_i \geq 0, \quad \min_{X_k \in \mathcal{X}_k} (2\bar{D}_i^k - I_n) X_k v_i \geq 0, \quad \forall i, k, \end{aligned}$$

where $v_i, w_i \in \mathbb{R}^{\bar{d}}$ for all $i \in [P_{\text{conv}}]$ and \bar{d} is the convolutional filter size. Moreover, X_k is the k^{th} patch of the data matrix X and \mathcal{X}_k is the corresponding perturbation set of the patch X_k . Furthermore, $\{\bar{D}_1, \dots, \bar{D}_{P_{\text{conv}}}\}$ is the set formed by all diagonal binary matrices that represent possible ReLU activation patterns associated with $\mathbf{M} := [X_1^\top \ \dots \ X_{P_{\text{conv}}}^\top]^\top$ and \bar{D}_i^k denotes the k^{th} \bar{d} -by- \bar{d} diagonal block of \bar{D}_i .

The next step would be to show that the above formulation is equivalent to a classic convex optimization. Note that each robust constraint is an LP subproblem that can be solved in closed form, which means that the robust constraints can be cast as equivalent classic constraints. When $\ell(\cdot)$ is the squared loss, the above equation becomes a robust second-order cone program (SOCP), which is known to be a convex optimization (similar to (D.3) of this work). Otherwise, if $\ell(\cdot)$ is monotonously increasing or decreasing in the CNN output $\hat{\mathbf{y}}$ (examples include the hinge loss and the binary cross-entropy loss), the inner maximization

problem

$$\arg \max_{X_k \in \mathcal{X}_k} \ell \left(\sum_{i=1}^{P_{\text{conv}}} \sum_{k=1}^K \bar{D}_i^k X_k (w_i - v_i), \mathbf{y} \right)$$

reduces to

$$\arg \max_{X_k \in \mathcal{X}_k} \sum_{i=1}^{P_{\text{conv}}} \sum_{k=1}^K \bar{D}_i^k X_k (w_i - v_i) \quad \text{or} \quad \arg \min_{X_k \in \mathcal{X}_k} \sum_{i=1}^{P_{\text{conv}}} \sum_{k=1}^K \bar{D}_i^k X_k (w_i - v_i),$$

which are LPs that can be solved in closed form. Substituting the closed-form solution yields the desired convex adversarial training formulations.

Similarly, for max pooling two-layer CNNs, the robust counterpart becomes (cf. Equation (7) of [24]):

$$\begin{aligned} \min_{\{v_i, w_i\}_{i=1}^{P_{\text{conv}}}} & \left(\max_{X_k \in \mathcal{X}_k} \ell \left(\sum_{i=1}^{P_{\text{conv}}} \sum_{k=1}^K \bar{D}_i^k X_k (w_i - v_i), \mathbf{y} \right) + \beta \sum_{i=1}^{P_{\text{conv}}} (\|v_i\|_2 + \|w_i\|_2) \right) \\ \text{s.t.} & \quad \min_{X_k \in \mathcal{X}_k} (2\bar{D}_i^k - I_n) X_k w_i \geq 0, \quad \min_{X_k \in \mathcal{X}_k} (2\bar{D}_i^k - I_n) X_k v_i \geq 0, \quad \forall i, k, \\ & \quad \min_{X_k \in \mathcal{X}_k} \bar{D}_i^k X_k v_i \geq \max_{X_j \in \mathcal{X}_j} \bar{D}_i^k X_j v_i, \quad \forall i, j, k, \\ & \quad \min_{X_k \in \mathcal{X}_k} \bar{D}_i^k X_k w_i \geq \max_{X_j \in \mathcal{X}_j} \bar{D}_i^k X_j w_i, \quad \forall i, j, k. \end{aligned}$$

where each additional robust constraint is an LP subproblem that can be solved in closed form.

The same robust optimization techniques can be applied to three-layer CNNs (cf. Equation (11) in [24]) and derive corresponding convex adversarial training formulations. In general, the convex standard training formulations for different NNs / CNNs share very similar structures. Therefore, many convex standard training formulations can be “robustified” by recasting as mini-max formulations. Whether these mini-max formulations can be reformed into classic convex optimizations depends on the specific structures of the problems. For CNNs with two or three layers considered in [24], such classic convex formulations can be derived.

Similarly, the ADMM splitting scheme, discussed in section 3, also applies to the above CNN formulations. The CNN training formulations can be similarly split into loss function terms, regularization terms, and linear inequality constraints.

D.3. ℓ_p norm-bounded perturbation set for hinge loss. Theorem 4.3 can be extended to the following ℓ_p norm-bounded perturbation set:

$$\tilde{\mathcal{X}} = \{X + \Delta \in \mathbb{R}^{n \times d} \mid \Delta = [\delta_1 \ \cdots \ \delta_n]^\top, \|\delta_k\|_p \leq \epsilon, \forall k \in [n]\}.$$

In the case of performing binary classification with a hinge-lossed ANN, the convex adversarial

training problem then becomes:

$$(D.5) \quad \min_{(v_i, w_i)_{i=1}^{\hat{P}}} \left(\frac{1}{n} \sum_{k=1}^n \left(1 - y_k \sum_{i=1}^{\hat{P}} d_{ik} x_k^\top (v_i - w_i) + \epsilon \cdot \left\| \sum_{i=1}^{\hat{P}} d_{ik} (v_i - w_i) \right\|_{p^*} \right)_+ \right. \\ \left. + \beta \sum_{i=1}^{\hat{P}} (\|v_i\|_2 + \|w_i\|_2) \right) \\ \text{s. t. } (2D_i - I_n)Xv_i \geq \epsilon \|v_i\|_{p^*}, \quad (2D_i - I_n)Xw_i \geq \epsilon \|w_i\|_{p^*}, \quad \forall i \in [\hat{P}]$$

where $D_1, \dots, D_{\hat{P}}$ are all distinct diagonal matrices associated with $\text{diag}([Xu \geq 0])$ for all possible $u \in \mathbb{R}^d$ and all $X + \Delta$ at the *boundary* of $\tilde{\mathcal{X}}$. Note that $\|\cdot\|_{p^*}$ is the dual norm of $\|\cdot\|_p$.

Appendix E. Proofs.

E.1. Proof of Theorem 2.2. We start by recasting the semi-infinite constraint of the dual formulation (2.3) as $\max_{\|u\|_2 \leq 1} |v^\top (Xu)_+| \leq \beta$ and obtain

$$\max_{\|u\|_2 \leq 1} |v^\top (Xu)_+| = \max_{\|u\|_2 \leq 1} |v^\top \text{diag}([Xu \geq 0])Xu| = \max_{i \in [P]} \left(\max_{\substack{\|u\|_2 \leq 1 \\ (2D_i - I_n)Xu \geq 0}} |v^\top D_i Xu| \right),$$

where the last equality holds by the definition of the D_i matrices: D_1, \dots, D_P are all distinct matrices that can be formed by $\text{diag}([Xu \geq 0])$ for some $u \in \mathbb{R}^d$. The constraint $(2D_i - I_n)Xu \geq 0$ is equivalent to $D_i Xu \geq 0$ and $(I_n - D_i)Xu \leq 0$, which forces $D_i = \text{diag}([Xu \geq 0])$ to hold.

Therefore, the dual formulation (2.3) can be recast as

$$(E.1) \quad \max_v -\ell^*(v) \quad \text{s. t. } \max_{\substack{\|u\|_2 \leq 1 \\ (2D_i - I_n)Xu \geq 0}} |v^\top D_i Xu| \leq \beta, \quad \forall i \in [P].$$

To form a tractable convex program that provides an approximation to (E.1), one can independently sample a subset of the diagonal matrices. One possible sampling procedure is presented in Algorithm 2.1. The sampled matrices, denoted as D_1, \dots, D_{P_s} , can be used to construct the relaxed problem:

$$(E.2) \quad d_{s1}^* = \max_v -\ell^*(v) \quad \text{s. t. } \max_{\substack{\|u\|_2 \leq 1 \\ (2D_h - I_n)Xu \geq 0}} |v^\top D_h Xu| \leq \beta, \quad \forall h \in [P_s].$$

The optimization problem (E.2) is convex with respect to v . [45] has shown that (E.1) has the same optimal objective as its dual problem (2.2). By following precisely the same derivation, it can be shown that (E.2) has the same optimal objective as (2.5) and $p_{s1}^* = d_{s1}^*$. Moreover, if an additional diagonal matrix D_{P_s+1} is independently randomly sampled to form (2.6), then we also have $p_{s2}^* = d_{s2}^*$, where

$$d_{s2}^* = \max_v -\ell^*(v) \quad \text{s. t. } \max_{\substack{\|u\|_2 \leq 1 \\ (2D_h - I_n)Xu \geq 0}} |v^\top D_h Xu| \leq \beta, \quad \forall h \in [P_s + 1].$$

Thus, the level of suboptimality of (E.2) compared with (E.1) is the level of suboptimality of (2.5) compared with (2.2). Notice that by introducing a slack variable $w \in \mathbb{R}$, (E.1) can be represented as an instance of the UCP with $n + 1$ optimization variables, defined in [16]:

$$\max_{v, w: w \leq -\ell^*(v)} w \quad \text{s. t.} \quad \max_{\substack{\|u\|_2 \leq 1 \\ (2D_i - I_n)Xu \geq 0}} |v^\top D_i Xu| \leq \beta, \quad \forall i \in [P].$$

The relaxed problem (E.2) can be regarded as a corresponding SCP. Suppose that w^*, v^* is a solution to the sampled convex problem (E.2). It can be concluded from [16, Theorem 1] and [17, Theorem 1] that if $P_s \geq \min \left\{ \frac{n+1}{\psi\xi} - 1, \frac{2}{\xi}(n+1 - \log \psi) \right\}$, then v^* satisfies the original constraints of the UCP (E.1) with high probability. Specifically, with probability no smaller than $1 - \xi$, we have

$$\mathbb{P} \left\{ D \in \mathcal{D} : \max_{\substack{\|u\|_2 \leq 1 \\ (2D - I_n)Xu \geq 0}} |v^{*\top} DXu| > \beta \right\} \leq \psi.$$

where \mathcal{D} denotes the set of all diagonal matrices that can be formed by $\text{diag}([Xu \geq 0])$ for some $u \in \mathbb{R}^d$, which is the set formed by D_1, \dots, D_P .

Since D_{P_s+1} is randomly sampled from \mathcal{D} , we have

$$\mathbb{P} \left\{ D \in \mathcal{D} : \max_{\substack{\|u\|_2 \leq 1 \\ (2D - I_n)Xu \geq 0}} |v^{*\top} DXu| > \beta \right\} = \mathbb{P} \left\{ \max_{\substack{\|u\|_2 \leq 1 \\ (2D_{P_s+1} - I_n)Xu \geq 0}} |v^{*\top} D_{P_s+1} Xu| > \beta \right\}$$

Thus, with probability no smaller than $1 - \xi$, it holds that

$$\mathbb{P} \left\{ \max_{\substack{\|u\|_2 \leq 1 \\ (2D_{P_s+1} - I_n)Xu \geq 0}} |v^{*\top} D_{P_s+1} Xu| > \beta \right\} \leq \psi.$$

Moreover, $d_{s_2}^* < d_{s_1}^*$ if and only if $|v^{*\top} D_{P_s+1} Xu| > \beta$ with $d_{s_2}^* = d_{s_1}^*$ otherwise. The proof is completed by noting that $p_{s_1}^* = d_{s_1}^*$ and $p_{s_2}^* = d_{s_2}^*$. \square

E.2. Proof of Theorem 3.1. We start by rewriting (3.2) as

$$(E.3) \quad \min_{v, s, u: s \geq 0} f_1(u) + f_2(v, s) \quad \text{s. t.} \quad E_1 u - E_2 \begin{bmatrix} v \\ s \end{bmatrix} = 0,$$

where $f_1(u) = \ell(Fu, y)$, $f_2(v, s) = \beta \|v\|_{2,1}$, $E_1 = \begin{bmatrix} I \\ G \end{bmatrix}$, and $E_2 = I$.

Furthermore, let $L(u, v, s, \nu, \lambda)$ denote the augmented Lagrangian:

$$L(u, v, s, \nu, \lambda) := f_1(u) + \beta \|v\|_{2,1} + \mathbb{I}_{\geq 0}(s) + \frac{\rho}{2} \left(\|u - v + \lambda\|_2^2 - \|\lambda\|_2^2 \right) + \frac{\rho}{2} \left(\|Gu - s + \nu\|_2^2 - \|\nu\|_2^2 \right)$$

Theorem 3.1 in [30] shows that the ADMM algorithm converges linearly when the objective satisfies seven conditions. We show that these conditions are all satisfied for (E.3) given the assumptions of Theorem 3.1 in this paper:

- (a) It can be easily shown that (E.3) attains a global solution because the feasible set of the equivalent problem (2.2) is non-empty.
- (b) We can then decompose $f_1(u)$ into $g_1(Fu) := \ell(Fu, y)$ and $h_1(u) := 0$ and define $h_2(\cdot) := f_2(\cdot)$. When the loss $\ell(\hat{y}, y)$ is convex with respect to \hat{y} , the functions $g_1(\cdot), h_1(\cdot), h_2(\cdot)$ are all convex and continuous.
- (c) When $\ell(\hat{y}, y)$ is strictly convex and continuously differentiable with a uniform Lipschitz continuous gradient with respect to \hat{y} , the function $g_1(\cdot)$ is strictly convex and continuously differentiable with a uniform Lipschitz continuous gradient.
- (d) The epigraph of $h_1(\cdot) = 0$ is a polyhedral set. Moreover, $h_2(v, s) = \|v\|_{2,1} = \sum_{i=1}^P (\|v_i\|_2 + \|w_i\|_2)$ by definition.
- (e) The constant function $h_1(\cdot)$ is trivially finite. Furthermore, for all u, v, s that make $L(u, v, s, \nu, \lambda)$ finite, it must hold that $f_1(u) < +\infty$, $v < +\infty$, and $s \geq 0$. Therefore, $h_2(\cdot)$ must be finite.
- (f) E_1 and E_2 both have full column rank since the identity matrix has full column rank.
- (g) When $u \rightarrow \infty$, we have $L(u, v, s, \nu, \lambda) \rightarrow \infty$. Hence, the solution to (3.3a) must be finite as long as the initial points $u^0, v^0, s^0, \lambda^0, \nu^0$ are finite. The solutions to (3.3b) and (3.3c) are also finite, since the closed-form solutions are derived in subsection 3.1. Therefore, the sequence $\{(u^k, v^k, s^k, \lambda^k, \nu^k)\}$ is finite. Thus, there exist finite $u_{\max}, v_{\max}, s_{\max}$ such that (E.3) is equivalent to the formulation below:

$$(E.4) \quad \min_{v, s, u} f_1(u) + f_2(v, s)$$

$$\text{s. t. } E_1 u - E_2 \begin{bmatrix} v \\ s \end{bmatrix} = 0, \quad \|u\|_\infty \leq u_{\max}, \quad \|v\|_\infty \leq v_{\max}, \quad \|s\|_\infty \leq s_{\max}.$$

Furthermore, the ADMM algorithm that solves (E.4) is equivalent to Algorithm 3.1. The feasible set of (E.4) is a compact polyhedral set formed by the ℓ_∞ norm constraints.

Thus, by the application of [30, Theorem 3.1], the desired result holds true when the step size γ_a is sufficiently small. \square

E.3. Proof of Theorem A.1. As discussed in Appendix A.2, strong duality holds between (A.1) and (A.4), as well as between (A.2) and (A.5). Here, we introduce a slack variable w and cast (A.4) as a canonical uncertain convex program with $n+1$ optimization variables and a linear objective, where n is the number of training data points:

$$\min_{(v, w) \in \mathcal{F}} w$$

$$\text{s. t. } f(v, w, u) := |v^\top (Xu)_+| - \beta \leq 0, \quad \forall u \in \mathcal{G}$$

$$\mathcal{F} = \{v \in \mathbb{R}^n, w \in \mathbb{R} \mid \|y - v\|_2^2 - 2w \leq 0\}$$

$$\mathcal{G} = \{u \mid \|u\|_2 = 1\}.$$

By leveraging [16, Theorem 1] and [17, Theorem 1], we can conclude that if $N \geq \min \left\{ \frac{n+1}{\psi\gamma} - 1, \frac{2}{\gamma}(n+1 - \log \psi) \right\}$, then with probability no smaller than $1 - \gamma$, the solution v^* to the randomized problem (A.5) satisfies $\mathbb{P}\{u : \|u\|_2 = 1, |v^{*\top}(Xu)_+| > \beta\} \leq \psi$. Since u_{N+1} is randomly generated on the Euclidean norm sphere via a uniform distribution, it holds that $\mathbb{P}\{|v^{*\top}(Xu_{N+1})_+| > \beta\} \leq \psi$.

Consider the following dual formulation with the newly sampled hidden neuron u_{N+1} included:

$$(E.5) \quad d_{s4}^* = \max_{v \in \mathbb{R}^n} -\ell^*(v) \quad \text{s.t.} \quad |v^\top(Xu_i)_+| \leq \beta, \quad \forall i \in [N+1].$$

Since (E.5) and (A.5) share the same objective, it holds that $d_{s4}^* < d_{s3}^*$ if and only if $|v^{*\top}(Xu_{N+1})_+| > \beta$ with $d_{s4}^* = d_{s3}^*$ otherwise. The proof is completed by recalling that $p_{s3}^* = d_{s3}^*$ and $p_{s4}^* = d_{s4}^*$ due to strong duality. \square

E.4. Details about the strong duality between (A.5) and (A.2).

E.4.1. General loss functions. In this part of the appendix, we explicitly derive the relationship between the optimal solutions $(\alpha_i^*)_{i=1}^N$ and v^* for the purpose of recovering the dual optimizers from the primal optimizers.

The SCP training formulation (A.2) is equivalent to the following constrained optimization:

$$(E.6) \quad \min_{r, (\alpha_i)_{i=1}^N} \ell(r, y) + \beta \sum_{i=1}^N |\alpha_i| \quad \text{s.t.} \quad r = \sum_{i=1}^N (Xu_i)_+ \alpha_i,$$

and a solution to (A.2) is also optimal for (E.6). The optimization (E.6) is then equivalent to the minimax problem

$$(E.7) \quad \min_{r, (\alpha_i)_{i=1}^N} \left(\max_v \ell(r, y) + \beta \sum_{i=1}^N |\alpha_i| + v^\top \left(\sum_{i=1}^N (Xu_i)_+ \alpha_i - r \right) \right).$$

The outer minimization is convex over r and $(\alpha_i)_{i=1}^N$, while the inner maximization is concave over v . Thus, by the Sion's minimax theorem [49], the optimization (E.7) is equivalent to:

$$\begin{aligned} & \max_v \left(\min_r \left(\ell(r, y) - v^\top r \right) + \min_{(\alpha_i)_{i=1}^N} \left(\beta \sum_{i=1}^N |\alpha_j| + v^\top \sum_{i=1}^N (Xu_j)_+ \alpha_j \right) \right) \\ &= \max_v \left(- \max_r \left(v^\top r - \ell(r, y) \right) \quad \text{s.t.} \quad |v^\top(Xu_i)_+| \leq \beta, \quad \forall i \in [N] \right) \\ &= \max_v -\ell^*(v) \quad \text{s.t.} \quad |v^\top(Xu_i)_+| \leq \beta, \quad \forall i \in [N], \end{aligned}$$

which is (A.5). The first equality holds because

$$\min_{(\alpha_i)_{i=1}^N} \left(\beta \sum_{i=1}^N |\alpha_j| + v^\top \sum_{i=1}^N (Xu_j)_+ \alpha_j \right) = \begin{cases} 0, & |v^\top(Xu_i)_+| \leq \beta, \quad \forall i \in [N], \\ \infty, & \text{otherwise.} \end{cases}$$

Therefore, with the optimal $(\alpha_i^*)_{i=1}^N$, one can calculate r^* via $r^* = \sum_{i=1}^N (Xu_i)_+ \alpha_i^*$, and recover v^* by solving the following LP:

$$v^* = \arg \max_v -v^\top r^* \quad \text{s. t.} \quad |v^\top (Xu_i)_+| \leq \beta, \quad \forall i \in [N].$$

E.4.2. Squared loss. In this part, we prove the relationship between $(\alpha_i^*)_{i=1}^N$ and v^* by deriving the Karush–Kuhn–Tucker (KKT) conditions for the special case when the squared loss is considered. In this case, the SCP training formulation (A.2) reduces to

$$\min_{(\alpha_i)_{i=1}^N} \frac{1}{2} \left\| \sum_{i=1}^N (Xu_i)_+ \alpha_i - y \right\|_2^2 + \beta \sum_{i=1}^N |\alpha_i|,$$

which is equivalent to

$$(E.8) \quad \min_{r, (\alpha_i)_{i=1}^N} \frac{1}{2} \|r\|_2^2 + \beta \sum_{i=1}^N |\alpha_i| \quad \text{s. t.} \quad r = \sum_{i=1}^N (Xu_i)_+ \alpha_i - y.$$

By introducing a dual vector variable $v \in \mathbb{R}^n$, we can write the Lagrangian of (E.8) as:

$$\begin{aligned} L_{\text{SCP}}(v, r, (\alpha_i)_{i=1}^N) &= \frac{1}{2} \|r\|_2^2 + \beta \sum_{i=1}^N |\alpha_i| + v^\top \left(\sum_{i=1}^N (Xu_i)_+ \alpha_i - y - r \right) \\ &= \left(\frac{1}{2} r^\top + v^\top \right) r + \left(\beta \sum_{i=1}^N |\alpha_i| + v^\top \sum_{i=1}^N (Xu_i)_+ \alpha_i \right) + v^\top y \end{aligned}$$

$L_{\text{SCP}}(v, r, (\alpha_i)_{i=1}^N)$ is smooth with respect to r . Thus, by the Lagrangian stationarity condition, at optimum, we must have $\nabla_r L(v^*, r^*, (\alpha_i^*)_{i=1}^N) = r^* + v^* = 0$. By the primal feasibility condition, we must have $r^* = \sum_{i=1}^N (Xu_i)_+ \alpha_i^* - y$. Thus, at the optimum, $v^* = y - \sum_{i=1}^N (Xu_i)_+ \alpha_i^*$.

E.5. Proof of Theorem 4.1. Before proceeding with the proof, we first present the following result borrowed from [45].

Lemma E.1. *For a given data matrix X and $(v_i, w_i)_{i=1}^P$, if $(2D_i - I_n)Xv_i \geq 0$ and $(2D_i - I_n)Xw_i \geq 0$ for all $i \in [P]$, then we can recover the corresponding ANN weights $(u_{v,w_j}, \alpha_{v,w_j})_{j=1}^{m^*}$ using the formulas in (2.4), and it holds that*

$$(E.9) \quad \begin{aligned} & \ell \left(\sum_{i=1}^P D_i X(v_i - w_i), y \right) + \beta \sum_{i=1}^P (\|v_i\|_2 + \|w_i\|_2) \\ &= \ell \left(\sum_{j=1}^{m^*} (Xu_{v,w_j})_+ \alpha_{v,w_j}, y \right) + \frac{\beta}{2} \sum_{j=1}^{m^*} (\|u_{v,w_j}\|_2^2 + \alpha_{v,w_j}^2). \end{aligned}$$

Theorem 2.1 implies that the non-convex cost function (2.1) has the same objective value as the following finite-dimensional convex optimization problem:

$$(E.10) \quad \begin{aligned} q^* &= \min_{(v_i, w_i)_{i=1}^P} \ell \left(\sum_{i=1}^P D_i X(v_i - w_i), y \right) + \beta \sum_{i=1}^P (\|v_i\|_2 + \|w_i\|_2) \\ \text{s. t.} \quad & (2D_i - I_n)Xv_i \geq 0, (2D_i - I_n)Xw_i \geq 0, \quad \forall i \in [P] \end{aligned}$$

where D_1, \dots, D_P are all of the matrices in the set of matrices \mathcal{D} , which is defined as the set of all distinct diagonal matrices $\text{diag}([Xu \geq 0])$ that can be obtained for all possible $u \in \mathbb{R}^d$. We recall that the optimal neural network weights can be recovered using (2.4).

Consider the following optimization problem:

$$(E.11) \quad \begin{aligned} \tilde{q}^* &= \min_{(v_i, w_i)_{i=1}^{\tilde{P}}} \ell \left(\sum_{i=1}^{\tilde{P}} D_i X(v_i - w_i), y \right) + \beta \sum_{i=1}^{\tilde{P}} (\|v_i\|_2 + \|w_i\|_2) \\ \text{s. t.} \quad & (2D_i - I_n)Xv_i \geq 0, (2D_i - I_n)Xw_i \geq 0, \quad \forall i \in [\tilde{P}] \end{aligned}$$

where additional D matrices, denoted as $D_{P+1}, \dots, D_{\tilde{P}}$, are introduced. These additional matrices are still diagonal with each entry being either 0 or 1, while they do not belong to \mathcal{D} . They represent ‘‘infeasible hyperplanes’’ that cannot be achieved by the sign pattern of Xu for any $u \in \mathbb{R}^d$.

Lemma E.2. *It holds that $\tilde{q}^* = q^*$, meaning that the optimization problem (E.11) has the same optimal objective as (E.10).*

The proof of Lemma E.2 is given in Appendix E.10.

The robust minimax training problem (4.1) considers an uncertain data matrix $X + \Delta$. Different values of $X + \Delta$ within the perturbation set \mathcal{U} can result in different D matrices. Now, we define $\hat{\mathcal{D}} = \bigcup_{\Delta} \mathcal{D}_{\Delta}$, where \mathcal{D}_{Δ} is the set of diagonal matrices for a particular Δ such that $X + \Delta \in \mathcal{U}$. By construction, we have $\mathcal{D}_{\Delta} \subseteq \hat{\mathcal{D}}$ for every Δ such that $X + \Delta \in \mathcal{U}$. Thus, if we define $D_1, \dots, D_{\hat{P}}$ as all matrices in $\hat{\mathcal{D}}$, then for every Δ with the property $X + \Delta \in \mathcal{U}$, the optimization problem

$$(E.12) \quad \begin{aligned} \min_{(v_i, w_i)_{i=1}^{\hat{P}}} \ell \left(\sum_{i=1}^{\hat{P}} D_i (X + \Delta)(v_i - w_i), y \right) + \beta \sum_{i=1}^{\hat{P}} (\|v_i\|_2 + \|w_i\|_2) \\ \text{s. t.} \quad (2D_i - I_n)(X + \Delta)v_i \geq 0, (2D_i - I_n)(X + \Delta)w_i \geq 0, \quad \forall i \in [\hat{P}] \end{aligned}$$

is equivalent to

$$\min_{(u_j, \alpha_j)_{j=1}^m} \ell \left(\sum_{j=1}^m ((X + \Delta)u_j)_+ \alpha_j, y \right) + \frac{\beta}{2} \sum_{j=1}^m (\|u_j\|_2^2 + \alpha_j^2)$$

as long as $m \geq \hat{m}^*$ with $\hat{m}^* = |\{i : v_i^*(\Delta) \neq 0\}| + |\{i : w_i^*(\Delta) \neq 0\}|$, where $(v_i^*(\Delta), w_i^*(\Delta))_{i=1}^{\hat{P}}$ denotes an optimal point to (E.12).

Now, we focus on the minimax training problem with a convex objective given by

$$(E.13) \quad \min_{(v_i, w_i)_{i=1}^{\hat{P}} \in \mathcal{F}} \left(\begin{array}{l} \max_{\Delta: X + \Delta \in \mathcal{U}} \ell \left(\sum_{i=1}^{\hat{P}} D_i(X + \Delta)(v_i - w_i), y \right) + \beta \sum_{i=1}^{\hat{P}} (\|v_i\|_2 + \|w_i\|_2) \\ \text{s. t. } (2D_i - I_n)(X + \Delta)v_i \geq 0, (2D_i - I_n)(X + \Delta)w_i \geq 0, \forall i \in [\hat{P}] \end{array} \right),$$

where \mathcal{F} is defined as:

$$\left\{ (v_i, w_i)_{i=1}^{\hat{P}} \mid \begin{array}{l} \exists \Delta : X + \Delta \in \mathcal{U} \\ \text{s. t. } (2D_i - I_n)(X + \Delta)v_i \geq 0, (2D_i - I_n)(X + \Delta)w_i \geq 0, \forall i \in [\hat{P}] \end{array} \right\}.$$

The introduction of the feasible set \mathcal{F} is to avoid the situation where the inner maximization over Δ is infeasible and the objective becomes $-\infty$, leaving the outer minimization problem unbounded.

Moreover, consider the following problem:

$$(E.14) \quad \min_{(v_i, w_i)_{i=1}^{\hat{P}}} \left(\begin{array}{l} \ell \left(\sum_{i=1}^{\hat{P}} D_i(X + \Delta_{v,w}^*)(v_i - w_i), y \right) + \beta \sum_{i=1}^{\hat{P}} (\|v_i\|_2 + \|w_i\|_2) \\ \text{s. t. } (2D_i - I_n)(X + \Delta_{v,w}^*)v_i \geq 0, (2D_i - I_n)(X + \Delta_{v,w}^*)w_i \geq 0, \forall i \in [\hat{P}] \end{array} \right)$$

where $\Delta_{v,w}^*$ is the optimal point for $\max_{\Delta: X + \Delta \in \mathcal{U}} \ell \left(\sum_{i=1}^{\hat{P}} D_i(X + \Delta)(v_i - w_i), y \right)$. Note that the inequality constraints are dropped for the maximization here compared to (E.13).

The optimization problem (E.13) gives a lower bound on (E.14). To prove this, we first rewrite (E.14) as:

$$\min_{(v_i, w_i)_{i=1}^{\hat{P}}} f((v_i, w_i)_{i=1}^{\hat{P}}), \text{ where } f((v_i, w_i)_{i=1}^{\hat{P}}) = \begin{cases} \ell \left(\sum_{i=1}^{\hat{P}} D_i(X + \Delta_{v,w}^*)(v_i - w_i), y \right) + \beta \sum_{i=1}^{\hat{P}} (\|v_i\|_2 + \|w_i\|_2), & \begin{array}{l} (2D_i - I_n)(X + \Delta_{v,w}^*)v_i \geq 0, \forall i \in [\hat{P}] \\ (2D_i - I_n)(X + \Delta_{v,w}^*)w_i \geq 0, \forall i \in [\hat{P}] \end{array} \\ +\infty, & \text{otherwise.} \end{cases}$$

Now, we analyze (E.13). Consider three cases:

Case 1: For some $(v_i, w_i)_{i=1}^{\hat{P}}$, $\Delta_{v,w}^*$ is optimal for the inner maximization of (E.13) and the inequality constraints are inactive. This happens whenever $\Delta_{v,w}^*$ is feasible for the particular choice of $(v_i, w_i)_{i=1}^{\hat{P}}$. In other words, $(2D_i - I_n)(X + \Delta_{v,w}^*)v_i \geq 0$ and $(2D_i - I_n)(X + \Delta_{v,w}^*)w_i \geq 0$

hold true for all $i \in [\hat{P}]$. For these $(v_i, w_i)_{i=1}^{\hat{P}}$, we have:

$$\begin{aligned} & \left(\begin{array}{l} \max_{\Delta: X+\Delta \in \mathcal{U}} \ell \left(\sum_{i=1}^{\hat{P}} D_i(X+\Delta)(v_i-w_i), y \right) + \beta \sum_{i=1}^{\hat{P}} (\|v_i\|_2 + \|w_i\|_2) \\ \text{s. t. } (2D_i - I_n)(X+\Delta)v_i \geq 0, (2D_i - I_n)(X+\Delta)w_i \geq 0, \forall i \in [\hat{P}] \end{array} \right) \\ & = \ell \left(\sum_{i=1}^{\hat{P}} D_i(X+\Delta_{v,w}^*)(v_i-w_i), y \right) + \beta \sum_{i=1}^{\hat{P}} (\|v_i\|_2 + \|w_i\|_2) \end{aligned}$$

Case 2: For some $(v_i, w_i)_{i=1}^{\hat{P}}$, $\Delta_{v,w}^*$ is infeasible, while some Δ within the perturbation bound satisfies the inequality constraints. Suppose that among the feasible Δ 's,

$$\begin{aligned} \tilde{\Delta}_{v,w}^* & = \arg \max_{\Delta: X+\Delta \in \mathcal{U}} \ell \left(\sum_{i=1}^{\hat{P}} D_i(X+\Delta)(v_i-w_i), y \right) + \beta \sum_{i=1}^{\hat{P}} (\|v_i\|_2 + \|w_i\|_2) \\ & \text{s. t. } (2D_i - I_n)(X+\Delta)v_i \geq 0, (2D_i - I_n)(X+\Delta)w_i \geq 0, \forall i \in [\hat{P}]. \end{aligned}$$

In this case,

$$\begin{aligned} & \left(\begin{array}{l} \max_{\Delta: X+\Delta \in \mathcal{U}} \ell \left(\sum_{i=1}^{\hat{P}} D_i(X+\Delta)(v_i-w_i), y \right) + \beta \sum_{i=1}^{\hat{P}} (\|v_i\|_2 + \|w_i\|_2) \\ \text{s. t. } (2D_i - I_n)(X+\Delta)v_i \geq 0, (2D_i - I_n)(X+\Delta)w_i \geq 0, \forall i \in [\hat{P}] \end{array} \right) \\ & = \ell \left(\sum_{i=1}^{\hat{P}} D_i(X+\tilde{\Delta}_{v,w}^*)(v_i-w_i), y \right) + \beta \sum_{i=1}^{\hat{P}} (\|v_i\|_2 + \|w_i\|_2) \end{aligned}$$

Case 3: For all other $(v_i, w_i)_{i=1}^{\hat{P}}$, the objective value is $+\infty$ since they do not belong to \mathcal{F} .

Therefore, (E.13) can be rewritten as

$$\min_{(v_i, w_i)_{i=1}^{\hat{P}}} g((v_i, w_i)_{i=1}^{\hat{P}}), \text{ where } g((v_i, w_i)_{i=1}^{\hat{P}}) = \begin{cases} \ell \left(\sum_{i=1}^{\hat{P}} D_i(X+\Delta_{v,w}^*)(v_i-w_i), y \right) + \beta \sum_{i=1}^{\hat{P}} (\|v_i\|_2 + \|w_i\|_2), & \begin{array}{l} (2D_i - I_n)(X+\Delta_{v,w}^*)v_i \geq 0, \forall i \in [\hat{P}] \\ (2D_i - I_n)(X+\Delta_{v,w}^*)w_i \geq 0, \forall i \in [\hat{P}] \end{array} \\ \ell \left(\sum_{i=1}^{\hat{P}} D_i(X+\tilde{\Delta}_{v,w}^*)(v_i-w_i), y \right) + \beta \sum_{i=1}^{\hat{P}} (\|v_i\|_2 + \|w_i\|_2), & \begin{array}{l} \exists j : (2D_j - I_n)(X+\Delta_{v,w}^*)v_j < 0 \\ \text{or } (2D_j - I_n)(X+\Delta_{v,w}^*)w_j < 0 \\ \exists \Delta : (2D_i - I_n)(X+\Delta)v_i \geq 0, \forall i \in [\hat{P}] \\ (2D_i - I_n)(X+\Delta)w_i \geq 0, \forall i \in [\hat{P}] \end{array} \\ +\infty, & \text{otherwise} \end{cases}$$

Hence, $g((v_i, w_i)_{i=1}^{\hat{P}}) = f((v_i, w_i)_{i=1}^{\hat{P}})$ for all $(v_i, w_i)_{i=1}^{\hat{P}}$ belonging to the first and the third cases. $g((v_i, w_i)_{i=1}^{\hat{P}}) < f((v_i, w_i)_{i=1}^{\hat{P}})$ for all $(v_i, w_i)_{i=1}^{\hat{P}}$ belonging to the second case. Thus, $\min_{(v_i, w_i)_{i=1}^{\hat{P}}} g((v_i, w_i)_{i=1}^{\hat{P}}) \leq \min_{(v_i, w_i)_{i=1}^{\hat{P}}} f((v_i, w_i)_{i=1}^{\hat{P}})$. This concludes that (E.13) is a lower bound to (E.14).

Let $(v_{\text{minimax}_i}^*, w_{\text{minimax}_i}^*)_{i=1}^{\hat{P}}$ denote an optimal point for (E.14). It is possible that for some $\Delta : X + \Delta \in \mathcal{U}$, the constraints $(2D_i - I_n)(X + \Delta)v_{\text{minimax}_i}^* \geq 0$ and $(2D_i - I_n)(X + \Delta)w_{\text{minimax}_i}^* \geq 0$ are not satisfied for all $i \in [\hat{P}]$. In light of Lemma E.1, at those Δ where such constraints are violated, the convex problem (E.14) does not reflect the cost of the ANN. For these infeasible Δ , the input-label pairs $(X + \Delta, y)$ can have a high cost in the ANN and potentially become the worst-case adversary. However, these Δ are ignored in (E.14) due to the infeasibility. Since adversarial training aims to minimize the cost over the worst-case adversaries generated upon the training data whereas (E.14) may sometimes miss the worst-case adversaries, (E.14) does not fully accomplish the task of adversarial training. In fact, by applying Theorem 2.1 and Lemma E.2, it can be verified that (E.13) and (E.14) are lower bounds to (4.1) as long as $m \geq \hat{m}^*$:

$$\begin{aligned} & \min_{(u_j, \alpha_j)_{j=1}^m} \left(\max_{\Delta: X + \Delta \in \mathcal{U}} \ell \left(\sum_{j=1}^m ((X + \Delta)u_j)_+ \alpha_j, y \right) + \frac{\beta}{2} \sum_{j=1}^m (\|u_j\|_2^2 + \alpha_j^2) \right) \\ & \geq \min_{(u_j, \alpha_j)_{j=1}^m} \ell \left(\sum_{j=1}^m ((X + \Delta_{v,w}^*)u_j)_+ \alpha_j, y \right) + \frac{\beta}{2} \sum_{j=1}^m (\|u_j\|_2^2 + \alpha_j^2) \\ & = \left(\min_{(v_i, w_i)_{i=1}^{\hat{P}}} \ell \left(\sum_{i=1}^{\hat{P}} D_i (X + \Delta_{v,w}^*) (v_i - w_i), y \right) + \beta \sum_{i=1}^{\hat{P}} (\|v_i\|_2 + \|w_i\|_2) \right. \\ & \quad \left. \text{s. t. } (2D_i - I_n)(X + \Delta_{v,w}^*)v_i \geq 0, (2D_i - I_n)(X + \Delta_{v,w}^*)w_i \geq 0, \forall i \in [\hat{P}] \right). \end{aligned}$$

To address the feasibility issue, we can apply robust optimization techniques ([14] section 4.4.2) and replace the constraints in (E.14) with robust convex constraints, which will lead to (4.4). Let $((v_{\text{rob}_i}^*, w_{\text{rob}_i}^*)_{i=1}^{\hat{P}}, \Delta_{\text{rob}}^*)$ denote an optimal point of (4.4) and let $(u_{\text{rob}_j}^*, \alpha_{\text{rob}_j}^*)_{j=1}^{\hat{m}^*}$ be the ANN weights recovered from $(v_{\text{rob}_i}^*, w_{\text{rob}_i}^*)_{i=1}^{\hat{P}}$ with (2.4), where \hat{m}^* is the number of nonzero weights. In light of Lemma E.1, since the constraints $(2D_i - I_n)(X + \Delta)v_{\text{rob}_i}^* \geq 0$ and $(2D_i - I_n)(X + \Delta)w_{\text{rob}_i}^* \geq 0$ for all $i \in [\hat{P}]$ apply to all $X + \Delta \in \mathcal{U}$, all $X + \Delta \in \mathcal{U}$ satisfy the equality

$$\begin{aligned} & \ell \left(\sum_{i=1}^{\hat{P}} D_i (X + \Delta) (v_{\text{rob}_i}^* - w_{\text{rob}_i}^*), y \right) + \beta \sum_{i=1}^{\hat{P}} (\|v_{\text{rob}_i}^*\|_2 + \|w_{\text{rob}_i}^*\|_2) \\ & = \ell \left(\sum_{j=1}^{\hat{m}^*} ((X + \Delta)u_{\text{rob}_j}^*)_+ \alpha_{\text{rob}_j}^*, y \right) + \frac{\beta}{2} \sum_{j=1}^{\hat{m}^*} (\|u_{\text{rob}_j}^*\|_2^2 + \alpha_{\text{rob}_j}^{*2}). \end{aligned}$$

Thus, since

$$\Delta_{\text{rob}}^* = \arg \max_{\Delta: X+\Delta \in \mathcal{U}} \ell \left(\sum_{i=1}^{\hat{P}} D_i(X + \Delta)(v_{\text{rob}_i}^* - w_{\text{rob}_i}^*), y \right) + \beta \sum_{i=1}^{\hat{P}} (\|v_{\text{rob}_i}^*\|_2 + \|w_{\text{rob}_i}^*\|_2),$$

we have

$$\Delta_{\text{rob}}^* = \arg \max_{\Delta: X+\Delta \in \mathcal{U}} \ell \left(\sum_{j=1}^{\hat{m}^*} ((X + \Delta)u_{\text{rob}_j}^*)_+ \alpha_{\text{rob}_j}^*, y \right) + \frac{\beta}{2} \sum_{j=1}^{\hat{m}^*} (\|u_{\text{rob}_j}^*\|_2^2 + \alpha_{\text{rob}_j}^{*2}),$$

giving rise to:

$$\begin{aligned} & \ell \left(\sum_{i=1}^{\hat{P}} D_i(X + \Delta_{\text{rob}}^*)(v_{\text{rob}_i}^* - w_{\text{rob}_i}^*), y \right) + \beta \sum_{i=1}^{\hat{P}} (\|v_{\text{rob}_i}^*\|_2 + \|w_{\text{rob}_i}^*\|_2) \\ &= \ell \left(\sum_{j=1}^{\hat{m}^*} ((X + \Delta_{\text{rob}}^*)u_{\text{rob}_j}^*)_+ \alpha_{\text{rob}_j}^*, y \right) + \frac{\beta}{2} \sum_{j=1}^{\hat{m}^*} (\|u_{\text{rob}_j}^*\|_2^2 + \alpha_{\text{rob}_j}^{*2}) \\ &= \max_{\Delta: X+\Delta \in \mathcal{U}} \ell \left(\sum_{j=1}^{\hat{m}^*} ((X + \Delta)u_{\text{rob}_j}^*)_+ \alpha_{\text{rob}_j}^*, y \right) + \frac{\beta}{2} \sum_{j=1}^{\hat{m}^*} (\|u_{\text{rob}_j}^*\|_2^2 + \alpha_{\text{rob}_j}^{*2}) \\ &\geq \min_{(u_j, \alpha_j)_{j=1}^{\hat{m}^*}} \left(\max_{\Delta: X+\Delta \in \mathcal{U}} \ell \left(\sum_{j=1}^{\hat{m}^*} ((X + \Delta)u_j)_+ \alpha_j, y \right) + \frac{\beta}{2} \sum_{j=1}^{\hat{m}^*} (\|u_j\|_2^2 + \alpha_j^2) \right) \end{aligned}$$

Therefore, (4.4) is an upper bound to (4.1). \square

E.6. Proof of Corollary 4.2. Define $E_i = 2D_i - I_n$ for all $i \in [\hat{P}]$. Note that each E_i is a diagonal matrix, and its diagonal elements are either -1 or 1. Therefore, for each $i \in [\hat{P}]$, we can analyze the robust constraint $\min_{\Delta: X+\Delta \in \mathcal{U}} E_i(X + \Delta)v_i \geq 0$ element-wise (for each data point). Let e_{ik} denote the k^{th} diagonal element of E_i and δ_{ik}^\top denote the k^{th} element of Δ that appears in the i^{th} constraint. We then have:

$$(E.15) \quad \left(\min_{\|\delta_{ik}\|_\infty \leq \epsilon} e_{ik}(x_k^\top + \delta_{ik}^\top)v_i \right) = \left(e_{ik}x_k^\top v_i + \min_{\|\delta_{ik}\|_\infty \leq \epsilon} e_{ik}\delta_{ik}^\top v_i \right) \geq 0$$

The minima of the above optimization problems are achieved at $\delta_{ik}^{**} = \epsilon \cdot \text{sgn}(e_{ik}v_i) = \epsilon \cdot e_{ik} \cdot \text{sgn}(v_i)$.

Note that as ϵ approaches 0, δ_{ik}^{**} and Δ_{rob}^* in Theorem 4.1 both approach 0, which means that the gap between the convex robust problem (4.10) and the non-convex adversarial training problem (4.8) diminishes. Substituting δ_{ik}^{**} into (E.15) yields that

$$\left(e_{ik}x_k^\top v_i - \epsilon \|e_{ik}v_i\|_1 \right) = \left(e_{ik}x_k^\top v_i - \epsilon \|v_i\|_1 \right) \geq 0.$$

Vertically concatenating $e_{ik}x_k^\top v_i - \epsilon \|v_i\|_1 \geq 0$ for all $i \in [\widehat{P}]$ gives the vectorized representation $E_i X v_i - \epsilon \|v_i\|_1 \geq 0$, which leads to (4.5). Since the constraints on w are exactly the same, we also have that $\min_{\Delta: X+\Delta \in \mathcal{U}} E_i(X+\Delta)w_i \geq 0$ is equivalent to $E_i X w_i - \epsilon \|w_i\|_1 \geq 0$ for all $i \in [\widehat{P}]$.

E.7. Proof of Theorem 4.3. The regularization term is independent of Δ . Thus, it can be ignored for the purpose of analyzing the inner maximization. Note that each D_i is diagonal, and its diagonal elements are either 0 or 1. Therefore, the inner maximization of (4.9) can be analyzed element-wise (cost of each data point).

The maximization problem of the loss at each data point is:

$$(E.16) \quad \max_{\|\delta_k\|_\infty \leq \epsilon} \left(1 - y_k \sum_{i=1}^P d_{ik}(x_k^\top + \delta_k^\top)(v_i - w_i) \right)_+$$

where d_{ik} is the k^{th} diagonal element of D_i and δ_k^\top is the k^{th} row of Δ . One can write:

$$\begin{aligned} & \max_{\|\delta_k\|_\infty \leq \epsilon} \left(1 - y_k \sum_{i=1}^P d_{ik}(x_k^\top + \delta_k^\top)(v_i - w_i) \right)_+ \\ &= \left(\max_{\|\delta_k\|_\infty \leq \epsilon} 1 - y_k \sum_{i=1}^P d_{ik}(x_k^\top + \delta_k^\top)(v_i - w_i) \right)_+ \\ &= \left(1 - y_k \sum_{i=1}^P d_{ik}x_k^\top(v_i - w_i) - \min_{\|\delta_k\|_\infty \leq \epsilon} \delta_k^\top y_k \sum_{i=1}^P d_{ik}(v_i - w_i) \right)_+. \end{aligned}$$

The optimal solution to $\min_{\|\delta_k\|_\infty \leq \epsilon} \delta_k^\top y_k \sum_{i=1}^P d_{ik}(v_i - w_i)$ is $\delta_{\text{hinge}_k}^* = -\epsilon \cdot \text{sgn}\left(y_k \sum_{i=1}^P d_{ik}(v_i - w_i)^\top\right)$, or equivalently:

$$\Delta_{\text{hinge}}^* = -\epsilon \cdot \text{sgn}\left(\sum_{i=1}^P D_i y(v_i - w_i)^\top\right).$$

By substituting $\delta_{\text{hinge}_k}^*$ into (E.16), the optimization problem (E.16) reduces to:

$$\begin{aligned} & \left(1 - y_k \sum_{i=1}^P d_{ik}x_k^\top(v_i - w_i) + \epsilon \left\| y_k \sum_{i=1}^P d_{ik}(v_i - w_i) \right\|_1 \right)_+ \\ &= \left(1 - y_k \sum_{i=1}^P d_{ik}x_k^\top(v_i - w_i) + \epsilon |y_k| \left\| \sum_{i=1}^P d_{ik}(v_i - w_i) \right\|_1 \right)_+. \end{aligned}$$

Therefore, the overall loss function is:

$$\frac{1}{n} \sum_{k=1}^n \left(1 - y_k \sum_{i=1}^P d_{ik}x_k^\top(v_i - w_i) + \epsilon |y_k| \left\| \sum_{i=1}^P d_{ik}(v_i - w_i) \right\|_1 \right)_+.$$

In the case of binary classification, $y = \{-1, 1\}^n$, and thus $|y_k| = 1$ for all $k \in [n]$. Therefore, the above is equivalent to

$$(E.17) \quad \frac{1}{n} \sum_{k=1}^n \left(1 - y_k \sum_{i=1}^P d_{ik} x_k^\top (v_i - w_i) + \epsilon \left\| \sum_{i=1}^P d_{ik} (v_i - w_i) \right\|_1 \right)_+$$

which is the objective of (4.10). This completes the proof. \square

E.8. Proof of Theorem D.1. We first exploit the structure of (D.3) and reformulate it as the following robust second-order cone program (SOCP) by introducing a slack variable $a \in \mathbb{R}$:

$$(E.18) \quad \begin{aligned} \min_{(v_i, w_i)_{i=1}^{\hat{P}}, a} \quad & a + \beta \sum_{i=1}^{\hat{P}} (\|v_i\|_2 + \|w_i\|_2) \\ \text{s. t.} \quad & (2D_i - I_n)Xv_i \geq \epsilon \|v_i\|_1, \quad (2D_i - I_n)Xw_i \geq \epsilon \|w_i\|_1, \quad \forall i \in [\hat{P}] \\ & \max_{\Delta: X+\Delta \in \mathcal{X}} \left\| \begin{bmatrix} \sum_{i=1}^{\hat{P}} D_i(X + \Delta)(v_i - w_i) - y \\ 2a - \frac{1}{4} \end{bmatrix} \right\|_2 \leq 2a + \frac{1}{4}, \quad \forall i \in [\hat{P}]. \end{aligned}$$

Then, we need to establish the equivalence between (E.18) and (D.4). To this end, we consider the constraints of (E.18) and argue that these can be recast as the constraints given in (D.4). One can write:

$$\begin{aligned} & \max_{\Delta: X+\Delta \in \mathcal{X}} \left\| \begin{bmatrix} \sum_{i=1}^{\hat{P}} D_i(X + \Delta)(v_i - w_i) - y \\ 2a - \frac{1}{4} \end{bmatrix} \right\|_2 \leq 2a + \frac{1}{4} \\ \iff & \max_{\|\delta_k\|_\infty \leq \epsilon, \forall k \in [n]} \left\| \begin{bmatrix} \sum_{i=1}^{\hat{P}} d_{i1}(x_1^\top - \delta_1^\top)(v_i - w_i) - y_1 \\ \sum_{i=1}^{\hat{P}} d_{i2}(x_2^\top - \delta_2^\top)(v_i - w_i) - y_2 \\ \vdots \\ \sum_{i=1}^{\hat{P}} d_{in}(x_n^\top - \delta_n^\top)(v_i - w_i) - y_n \\ 2a - \frac{1}{4} \end{bmatrix} \right\|_2 \leq 2a + \frac{1}{4} \\ \iff & \max_{\|\delta_k\|_\infty \leq \epsilon, \forall k \in [n]} \left(\sum_{k=1}^n \left(\sum_{i=1}^{\hat{P}} d_{ik}(x_k^\top - \delta_k^\top)(v_i - w_i) - y_k \right)^2 + \left(2a - \frac{1}{4} \right)^2 \right)^{\frac{1}{2}} \leq 2a + \frac{1}{4} \end{aligned}$$

where d_{ik} is the k^{th} diagonal element of D_i and δ_k^\top is the k^{th} row of Δ . The above constraints can be rewritten by introducing slack variables $z \in \mathbb{R}^{n+1}$ as

$$\begin{aligned} z_k &\geq \left| \sum_{i=1}^{\hat{P}} d_{ik} x_k^\top (v_i - w_i) - y_k \right| + \epsilon \left\| \sum_{i=1}^{\hat{P}} d_{ik} (v_i - w_i) \right\|_1, \quad \forall k \in [n] \\ z_{n+1} &\geq \left| 2a - \frac{1}{4} \right|, \quad \|z\|_2 \leq 2a + \frac{1}{4}. \end{aligned}$$

\square

E.9. Proof of Theorem 4.4. The inner maximization of (4.12) can be analyzed separately for each y_k . For every index k such that $y_k = 0$, it holds that $\sum_{k=1}^n (-2\hat{y}_k y_k + \log(e^{2\hat{y}_k} + 1))$ monotonously increases with respect to \hat{y}_k . Thus, we need to find δ_k that maximizes \hat{y}_k in order to maximize the objective. Therefore, the worst-case adversary δ_k^* is

$$(E.19) \quad \delta_{k:y_k=0}^* = \arg \max_{\|\delta_k\|_\infty \leq \epsilon} \left(\sum_{i=1}^{\hat{P}} d_{ik} \delta_k^\top (v_i - w_i) \right) = \epsilon \cdot \operatorname{sgn} \left(\sum_{i=1}^{\hat{P}} d_{ik} (v_i - w_i)^\top \right).$$

For each index k such that $y_k = 1$, it holds that $\sum_{k=1}^n (-2\hat{y}_k y_k + \log(e^{2\hat{y}_k} + 1))$ monotonously decreases with respect to \hat{y}_k . Thus, we need to minimize \hat{y}_k . Therefore,

$$(E.20) \quad \delta_{k:y_k=1}^* = \arg \min_{\|\delta_k\|_\infty \leq \epsilon} \left(\sum_{i=1}^{\hat{P}} d_{ik} \delta_k^\top (v_i - w_i) \right) = -\epsilon \cdot \operatorname{sgn} \left(\sum_{i=1}^{\hat{P}} d_{ik} (v_i - w_i)^\top \right).$$

The two cases can be combined as $\delta_k^* = -\epsilon \cdot \operatorname{sgn} \left((2y_k - 1) \sum_{i=1}^{\hat{P}} d_{ik} (v_i - w_i)^\top \right)$. Concatenating $\delta_1^*, \dots, \delta_n^*$ back into the matrix form yields the worst-case perturbation matrix $\Delta_{\text{BCE}}^* = -\epsilon \cdot \operatorname{sgn} \left((2y - 1) \sum_{i=1}^{\hat{P}} D_i (v_i - w_i)^\top \right)$.

Moreover, notice that the objective is separable based on those k such that $y_k = 0$ and those k such that $y_k = 1$:

$$(E.21) \quad \begin{aligned} & \sum_{k=1}^n \left(-2\hat{y}_k y_k + \log(e^{2\hat{y}_k} + 1) \right) \\ &= \sum_{k:y_k=1} \left(-2\hat{y}_k + \log(e^{2\hat{y}_k} + 1) \right) + \sum_{k:y_k=0} \log(e^{2\hat{y}_k} + 1) \\ &= \sum_{k:y_k=1} \log \left(\frac{e^{2\hat{y}_k} + 1}{e^{2\hat{y}_k}} \right) + \sum_{k:y_k=0} \log(e^{2\hat{y}_k} + 1) \\ &= \sum_{k:y_k=1} \log(e^{-2\hat{y}_k} + 1) + \sum_{k:y_k=0} \log(e^{2\hat{y}_k} + 1) \\ &= \sum_{k:y_k=1} \log \left(\exp \left(-2 \sum_{i=1}^{\hat{P}} d_{ik} x_k^\top (v_i - w_i) + 2\epsilon \cdot \left\| \sum_{i=1}^{\hat{P}} d_{ik} (v_i - w_i) \right\|_1 \right) + 1 \right) \end{aligned}$$

$$(E.22) \quad \begin{aligned} & + \sum_{k:y_k=0} \log \left(\exp \left(2 \sum_{i=1}^{\hat{P}} d_{ik} x_k^\top (v_i - w_i) + 2\epsilon \cdot \left\| \sum_{i=1}^{\hat{P}} d_{ik} (v_i - w_i) \right\|_1 \right) + 1 \right) \\ &= \sum_{k=1}^n \log \left(\exp \left(2 \left((2y_k - 1) \sum_{i=1}^{\hat{P}} d_{ik} x_k^\top (v_i - w_i) + \epsilon \cdot \left\| \sum_{i=1}^{\hat{P}} d_{ik} (v_i - w_i) \right\|_1 \right) \right) + 1 \right) \\ &= \sum_{k=1}^n f \circ g_k(\{v_i, w_i\}_{i=1}^{\hat{P}}) \end{aligned}$$

where (E.21) and (E.22) are obtained by substituting in (E.19) and (E.20), and $f(\cdot)$, $g(\cdot)$ are defined in (4.13). Substituting the term $\sum_{k=1}^n (-2\hat{y}_k y_k + \log(e^{2\hat{y}_k} + 1))$ in (4.12) with the term $\sum_{k=1}^n f \circ g_k(\{v_i, w_i\}_{i=1}^{\tilde{P}})$ yields the formulation (4.13). Since the function $f(\cdot)$ is convex non-decreasing and $g(\cdot)$ is convex, the optimization (4.13) is convex. \square

E.10. Proof of Lemma E.2. According to [45], recovering the ANN weights by substituting (2.4) into (E.10) leads to

$$\begin{aligned} q^* &= \min_{(v_i, w_i)_{i=1}^P} \ell \left(\sum_{i=1}^P D_i X(v_i - w_i), y \right) + \beta \sum_{i=1}^P (\|v_i\|_2 + \|w_i\|_2) \\ &= \min_{(u_j, \alpha_j)_{j=1}^{m^*}} \ell \left(\sum_{j=1}^{m^*} (X u_j)_+ \alpha_j, y \right) + \frac{\beta}{2} \sum_{j=1}^{m^*} (\|u_j\|_2^2 + \alpha_j^2) \end{aligned}$$

Similarly, we can recover the network weights from the solution $(\tilde{v}_i^*, \tilde{w}_i^*)_{i=1}^{\tilde{P}}$ of (E.11) using

$$(E.23) \quad (\tilde{u}_{j_{1i}}, \tilde{\alpha}_{j_{1i}}) = \left(\frac{\tilde{v}_i^*}{\sqrt{\|\tilde{v}_i^*\|_2}}, \sqrt{\|\tilde{v}_i^*\|_2} \right), \quad (\tilde{u}_{j_{2i}}, \tilde{\alpha}_{j_{2i}}) = \left(\frac{\tilde{w}_i^*}{\sqrt{\|\tilde{w}_i^*\|_2}}, -\sqrt{\|\tilde{w}_i^*\|_2} \right), \quad \forall i \in [\tilde{P}].$$

Unlike in (2.4), zero weights are not discarded in (E.23). For simplicity, we use $\tilde{u}_1, \dots, \tilde{u}_{\tilde{m}^*}$ to refer to the hidden layer weights and use $\tilde{\alpha}_1, \dots, \tilde{\alpha}_{\tilde{m}^*}$ to refer to the output layer weights recovered using (E.23). Since $(\tilde{v}_i^*, \tilde{w}_i^*)_{i=1}^{\tilde{P}}$ is a solution to (E.11), it satisfies $(2D_i - I_n)X\tilde{v}_i^* \geq 0$ and $(2D_i - I_n)X\tilde{w}_i^* \geq 0$ for all $i \in [\tilde{P}]$. Thus, we can apply Lemma E.1 to obtain:

$$\begin{aligned} \tilde{q}^* &= \ell \left(\sum_{i=1}^{\tilde{P}} D_i X(\tilde{v}_i^* - \tilde{w}_i^*), y \right) + \beta \sum_{i=1}^{\tilde{P}} (\|\tilde{v}_i^*\|_2 + \|\tilde{w}_i^*\|_2) \\ &= \ell \left(\sum_{j=1}^{\tilde{m}^*} (X \tilde{u}_j^*)_+ \alpha_j, y \right) + \frac{\beta}{2} \sum_{j=1}^{\tilde{m}^*} (\|\tilde{u}_j^*\|_2^2 + \tilde{\alpha}_j^{*2}) \\ &\geq \min_{(u_j, \alpha_j)_{j=1}^{\tilde{m}^*}} \ell \left(\sum_{j=1}^{\tilde{m}^*} (X u_j)_+ \alpha_j, y \right) + \frac{\beta}{2} \sum_{j=1}^{\tilde{m}^*} (\|u_j\|_2^2 + \alpha_j^2) \end{aligned}$$

Since $\tilde{P} \geq P$, $m^* \leq 2\tilde{P}$ and $\tilde{m}^* = 2\tilde{P}$, we have $\tilde{m}^* \geq m^*$. Therefore, according to Section 2 and Theorem 6 of [45], we have:

$$\begin{aligned} q^* &= \min_{(u_j, \alpha_j)_{j=1}^{m^*}} \ell \left(\sum_{j=1}^{m^*} (X u_j)_+ \alpha_j, y \right) + \frac{\beta}{2} \sum_{j=1}^{m^*} (\|u_j\|_2^2 + \alpha_j^2) \\ &= \min_{(u_j, \alpha_j)_{j=1}^{\tilde{m}^*}} \ell \left(\sum_{j=1}^{\tilde{m}^*} (X u_j)_+ \alpha_j, y \right) + \frac{\beta}{2} \sum_{j=1}^{\tilde{m}^*} (\|u_j\|_2^2 + \alpha_j^2) \leq \tilde{q}^*. \end{aligned}$$

The above inequality $q^* \leq \tilde{q}^*$ shows that an ANN with more than m neurons in the hidden layer will yield the same loss as the ANN with m neurons when optimized.

Note that (E.11) can always attain q^* by simply substituting in the optimal solution of (E.10) and assigning zeros to all other additional v_i and w_i , implying that $q^* \geq \tilde{q}^*$. Since q^* is both an upper bound and a lower bound on \tilde{q}^* , we have $\tilde{q}^* = q^*$, proving that as long as all matrices in \mathcal{D} are included, the existence of redundant matrices does not change the optimal objective value. \square